A Life Cycle Simulation Model for Exploring Causes of Population Change in Alewife (*Alosa pseudoharengus*)

Gary A. Nelson[1*], Benjamin I. Gahagan[1], Michael P. Armstrong[1], Adrian Jordaan[2], Alison Bowden[3]

[1]Massachusetts Division of Marine Fisheries, 30 Emerson Avenue, Gloucester, MA 01930
[2]Department of Environmental Conservation, University of Massachusetts, Amherst, MA 01003
[3]The Nature Conservancy, 99 Bedford Street, Suite 500, Boston, Massachusetts 02111

*Corresponding author
Email address: gary.nelson@mass.gov

Abstract

Over the last two decades, major changes in abundance and population characteristics of Alewife (*Alosa pseudoharengus*), an anadromous herring species, have been observed along the US Atlantic coast. Loss of spawning habitat, bycatch mortality in the directed pelagic fisheries, increased predation mortality by rebounding predators such as Striped Bass, changes in water flow and temperature affecting recruitment success, changes in ocean thermal habitat and direct and indirect effects of changes in zooplankton community have been expounded by different researchers as putative hypotheses for population changes in Alewife. Unfortunately, long-term, concurrently-measured time series of regional factors and direct measures of biological processes needed to elucidate underlying causes are severely lacking for Alewife. Therefore, we developed, calibrated and validated a mechanistic, spatially-explicit, full life-cycle simulation model that can be used to explore population responses of Alewife to various exogeneous drivers. Daily processes such as spawning, recruitment, mortality, exploitation, predation and movements are generated by using empirically-derived deterministic and stochastic relationships and time-series of environmental data linked to specific life stages. We demonstrate the use of the model as an investigative tool by simulating three hypotheses and comparing model results to observed trends in Alewife populations from southern New England.

1. Introduction

Alewife (*Alosa pseudoharengus*) is an ecologically-important, migratory, anadromous herring species that ranges along the Atlantic coast from Labrador to South Carolina (Loesch 1987). Alewife spend most of their life at sea but enter freshwater in spring to spawn (primarily in lakes and ponds). After spawning, Alewife adults exit the freshwater system and are presumed to move offshore and northward to summer feeding grounds. The large-scale movement makes them important forage for many marine and freshwater fish predators such as striped bass (*Morone saxatilis*), cod (*Gadus morhua*), and yellow perch (*Perca flavescens*)(Loesch, 1987) as well as birds (Dalton et al., 2009). In addition, they are a key link in the transfer of nutrients between freshwater to marine systems (Mullen et al., 1986; Walters et al., 2009; Dias et al., 2019).

Over the last two decades, major changes in abundance and population characteristics of Alewife have been observed along the US Atlantic coast (Schimdt et al., 2003; ASMFC 2017). In southern New England, dramatic increases in run abundances of Alewife occurred during the 1980s and 1990s, but precipitous declines occurred after 2000 (Figure 1A)(Nelson et al., 2011; Davis and Schultz, 2009). In addition, declines in mean body size (Figure 1B) and mean age (Figure 1C) of Alewife have been observed in Massachusetts rivers since the 1980s and currently are about 20-25 mm smaller than in the past (Nelson et al., 2011; ASMFC, 2017). Concurrently, increases in total mortality and decreases in recruiting age classes have been noted (Figure 1D)(Nelson et al., 2011; ASMFC, 2017).

Researchers have expounded many hypotheses to explain the observed changes in population characteristics. Hall et al. (2012) suggested that historical loss of spawning habitat and productivity due to damming of rivers has decreased the resiliency of Alewife populations to

82 increases in mortality sources such as harvesting. Direct in-river harvest has varied over time,
83 but currently occurs only in Maine and a handful of other locations with approved management
84 plans (ASMFC 2017). Moratoriums limit direct harvest throughout much of the species range.
85 However, the occurrences of large incidental catches (bycatch) of Alewife in Atlantic Herring
86 (*Clupea harengus*) and Atlantic Mackerel (*Scomber scombrus*) fisheries off Southern New
87 England during fall and winter (Cournane et al. 2013) have been identified by many (ASMFC
88 2012; Hasselman et al. 2016; Palkovacs et al. 2013) as a potential cause of changes in
89 abundances. Increased predation mortality by rebounding predator populations like Striped
90 Bass (*Morone saxatilis*) and Double-Crested Cormorants (*Phalacrocorax auritus*) have been
91 suggested as a major cause as well (Dalton et al., 2009; Davis et al., 2012; Savoy and Crecco,
92 1995; Schmidt et al., 2003). Other putative causes include variability in water temperature and
93 flow affecting recruitment success (Tommasi et al., 2014), changes in ocean thermal habitat
94 (Lynch et al. 2015; Nye et al. 2009) and direct and indirect effects of changes in zooplankton and
95 phytoplankton composition (Kane 2011; Pershing et al., 2005), as a result of climate change.
96 With many factors potentially affecting growth and survival, the complex nature of interactions
97 between biotic and environmental factors, and regional differences in some of those factors,
98 such as bycatch (Hasselman et al., 2016), it seems unlikely that a single factor is responsible for
99 the observed changes in Alewife populations. Unfortunately, long-term, concurrently-measured
100 time series of regional factors and direct measures of biological processes (e.g., egg survival,
101 predation rates, etc.) needed to elucidate underlying causes are severely lacking for Alewife.
102 In the absence of long-term datasets, one method commonly used to understand complex
103 biological and environmental relationships in natural systems is simulation modeling. Through
104 simulation, population responses to changes in hypothesized causal mechanisms can be explored

and evaluated with models of population dynamics (Archambault et al., 2018; Watermeyer et al., 2018; Zeug et al., 2012). Such models allow researchers to conceptualize, describe and analyze population behavior and ask "what-if" questions about the real system. Because Alewife populations are under the influence of multiple environmental, predator and anthropogenic pressures at all life stages, exploration of causal factors requires the development of a life cycle model that incorporates relationships between the stressors and population dynamics. In this paper, we present a comprehensive, mechanistic, spatially-explicit, full life-cycle simulation model for predicting population responses of Alewife. The model is the first of its kind as processes such as spawning, recruitment, mortality, exploitation, predation and movements are generated by using empirically-derived deterministic and stochastic relationships and time-series of environmental data are linked to specific life stages. In addition, we validate the model by comparing predictions to data from published and unpublished studies not used in model calibration, and show a detailed analysis of model sensitivities. Further, we demonstrate how the model may be used as an investigative tool for exploring hypotheses related to population changes in Alewife.

2. Methodology

2.1. General Model Description

The simulation model, developed in *R* (R Development Core Team, 2016), is empirically-based and incorporates egg, yolk-sac larval, post-larval/young-of-the-year, juvenile (immature fish of age 1 and greater) and adult (mature) stages of Alewife, although the amount of detail varies among stages. The population structure is sex-specific, length-platoon (Goodyear 1989; 2002) and age-based meaning groups of individuals of a particular sex, length platoon, and

128 age are followed through time over a daily time step. The platoon-based structure is an
129 intermediate stance between all individuals of the same age progressing identically (age-based
130 model) and every individual have its own life path (individual-based model). The model is
131 specified to represent the regional (ocean, estuary, river and lake), sex (female and male),
132 maturity and length differences in population dynamics (Figure 2A). The model was developed
133 to differentiate among habitats such that different causes of mortality and changes in productivity
134 can be examined. Specifically, in the ocean, juveniles and adults grow and die due to length-
135 related natural mortality and can experience size-selective, seasonal bycatch mortality from the
136 bottom trawl and mid-water trawl Atlantic herring fisheries. Mature adults migrate to lake
137 spawning habitat through estuary and river systems (where they can experience in-river harvest)
138 and undergo temperature-dependent batch spawning in the lake. Once spawning is completed,
139 adults return to the ocean depending on the duration spent in each system (Figure 2A).
140 The sub-model for age-0 dynamics is more detailed (Figure 2B). Daily batches of eggs
141 laid by all spawning individuals on the same day are followed through time. Temperature
142 determines development of egg and yolk-sac stages. First-feeding post-larvae experience initial
143 carrying capacity mortality and length-based natural mortality occurs thereafter. In the post-
144 larval/young-of-the-year (YOY) stage, a bioenergetics model is used to grow length platoons
145 using area temperatures as input and platoons emigrate based on size, temperature and rainfall.
146 Duration of time spent in river and estuary is dependent on swimming speed and system length.
147 All YOY are moved to the ocean region by January 1 of the following year.
148
149 *2.2 Juvenile/Adult Sub-Model*

150 In this section we provide full details of the model processes for the juvenile/adult sub-
151 model. All functional relationships are empirically-based and were taken from literature or
152 estimated from unpublished field data. Descriptions of indexes are listed in Table 1, definitions
153 of mathematical symbols are given in Table 2, and mathematical equations are listed in Table 3.
154 Parameter values are listed in Appendix Table A. The general order of daily processes for the
155 juvenile/adult model is:
156 *Movement among habitats (when applicable)→ Harvest/bycatch (fishing) mortality+Natural*
157 *mortality→Growth*
158
159 *2.2.1 Population Structure*
160 The female and male components of juvenile and adult subgroups were defined as having
161 nine ages (last age is a plus-group) and one-hundred length platoons in each age. The number of
162 length platoons was selected to obtain similar length frequency statistics (mean, standard
163 deviation and percentiles) as an individual-based model that used identical growth rates.
164
165 *2.2.2 Population Dynamics*
166 The number of individuals (N) of juvenile and adult fish is modeled using an exponential
167 decay equation specific to each region. While in the ocean, the number of fish surviving to the
168 start of day d is dependent on bycatch mortality (F) and natural mortality (M) during day d-1
169 (Eq. JA.1). Length-dependent daily bycatch mortality is calculated from annual instantaneous
170 bycatch mortality, user-specified proportions representing monthly fractions of the fishing
171 pattern, and the number of days in a month. The daily F is further sub-divided in two fleet-
172 specific daily bycatch mortalities based on landings ratios derived from Massachusetts Division
173 of Marine Fisheries (MADMF) port sampling of the Atlantic herring fisheries (Eq. JA.2).

Length-dependent, fleet-specific daily *F* is calculated by multiplying fleet-specific daily *F* and fleet-specific selectivity-at-length values developed by using an equilibrium model and observed bycatch lengths (Supplementary Document Section 1).

Natural mortality experienced by fishes is often related to body size or weight (Pepin 1991; Lorenzen, 1996). For Alewife, we developed an equation to predict daily *M* from length that is used for all juvenile and adult fish regardless of sex or region. The Lorenzen (1996) weight-based *M* equation was altered to predict annual mortality from length by substituting a weight-length equation for Alewife sampled as bycatch (Eq. JA.3). Length-dependent daily *M* is calculated by dividing the estimated annual *M* from length by the days in a year (365). Migrating adult fish experience the same natural mortality rate while in estuary, river and lake systems, but additional harvest and predation mortality can occur in the river. Regional multipliers (δ) are available in Eqs. JA.1, JA.4 and JA.5 to adjust rates up or down if required. In the simulation, regional multipliers of 1.0 are used to obtain a baseline annual M of about 0.6 for ages 5-8 similar to Gibson and Myers (2003).

2.2.3 Growth

The body length of platoon *p* on day *d* is calculated from body length at the start of day *d-1* and the daily growth increment (ΔL) (Eq. JA.6). ΔL is calculated from the annual growth increment formulation of the von Bertalanffy equation (Quinn and Deriso, 1999)(Eq. JA.7) and a sine function that generates the fraction of annual growth that occurs on a given day of the year (Eq. JA.8). Because Alewife exhibit sexually-dimorphic growth rates, separate growth equations for female and male Alewife were derived (Supplementary Document Section 2).

197 *2.2.4 Movement of Mature Fish to Estuary*

198 Based on the University of Rhode Island Graduate School of Oceanography Fish Trawl
199 Survey (https://web.uri.edu/fishtrawl/), mature Alewife appear to enter an estuary during late
200 February-early March. To move mature fish from the ocean to the estuary region, the day of
201 movement (*ES*) is selected from a uniform distribution (Appendix A). All mature fish move
202 together at the beginning of the selected day.

203

204 *2.2.5 Movement of Mature Fish to River*

205 Mature fish move through the freshwater system (into river and lake and return) using
206 prior knowledge of temperature, swimming speed (v) and system length, and estimated spawning
207 duration is determined when a platoon enters the lake. The number of fish that move into the
208 river, and those that remain in the estuary, at the beginning of day d are calculated according to
209 Eqs. JA.9 and JA.10, respectively, where θ_d is the fraction migrating on day d. The mechanisms
210 controlling when and how many alewife enter a river are unknown; therefore, θ_d is simulated
211 over time. For a given year, the start day of a run is the day on which the average of the current
212 daily temperature and temperatures from the prior four days is $\geq$ 9.5^{o}C. This method was
213 developed to obtain start days within the ranges observed in the Monument River, MA (e.g.,
214 Sheppard and Bednarski 2015). The peak day and length of a run are selected randomly from
215 uniform distributions (run peak: day 114-137; run length: 63-87 days). The start, peak and end
216 days are input parameters to a triangle distribution (Eq. JA.11) and auto-correlated errors are
217 added to the probabilities to mimic the fluctuating run trends observed in the Monument River
218 (Eq. JA.12). The initial probabilities (p^{*}_{d} s) are standardized to 1 (Eq. JA.13). To ensure that all
219 fish move into the river by the end of the run, θ_d is determined sequentially following Eq. JA.14.

220 The duration spent in the river (*rdur*) is determined by the river length, swimming speed and
221 average body length (Eq. JA.15).
222 *2.2.6 Movement of Mature Adults from River to Lake*
223 The day of lake entry for each migrant group is calculated as the river entry day plus the
224 time spent by the group in the river, and the entire group of fish moves together on that day.
225
226 *2.2.7 Duration Spent in Lake*
227 The duration that a group spends in the lake (*sdur*) depends on when it enters during the
228 run (Kissel 1974). The duration is generated from an exponential equation fitted to Kissel (1974)
229 data (Eq. JA.16) and random deviates (Eq. JA.17) are added to mimic the distributions of
230 durations.
231
232 *2.2.8 Reproduction*
233 For a group of fish entering the lake, spawning activity commences on the day when the
234 lake temperature reaches a minimum temperature threshold (10.5 ºC; Fay et al., 1983). If a
235 group of fish arrives before the minimum threshold is reached, the first day of spawning is
236 registered as the day when the minimum threshold is reached. If a group of fish arrives after the
237 minimum threshold is reached, the first day of spawning (*spday*) is selected randomly from 4 to
238 8 days after lake entry as long as lake duration is >8 days; otherwise, the first spawning day is
239 the day of lake entry. The number of spawning events is determined by dividing the days spent
240 in the lake by the average number of days between spawned egg batches (*Bdur)*. The next
241 spawning event is determined by B_{dur}+1 + *d* (day of spawning). Spawning occurs at the

beginning of the day and the total number of eggs spawned by a group on a given day (E_d) is calculated by Eq. JA.18 using literature values and a weight-length equation (Eq. JA.19).

2.2.9 Lake Emigration

The day on which adult moves out of the lake is calculated as lake entry day plus the number of days spent in the lake.

2.2.10 River and Estuary Emigration

The day on which movement to the estuary occurs is calculated as the river entry day plus *rdur*. The day on which movement to the ocean occurs is calculated as the river exit day plus the the time spent in the estuary (*edur*). *edur* is calculated by using the same equation for *rdur* except estuary length (a user-specified parameter that can be adjusted to retain fish longer) is used (Eq. JA.15). Any fish remaining in the estuary are automatically moved to the ocean on day 1 of the following year.

2.2.11 Juvenile Maturation

On day 1 of each year, a fraction of juveniles in each platoon is matured according to sex-specific proportion-mature-at-length relationships (Eq. JA.20). The maturity-at-length relationships were estimated following Maki et al. (2001) using scale age and spawning check data collected from Monument River Alewife (full details in Supplementary Document Section 3).

2.3 Egg, Yolk-sac Larval, Post-larval/YOY Sub-model

In this section, we provide full details of the model processes. Definitions of mathematical symbols and mathematical equations for the egg-YOY sub-model are given in Tables 4 and 5, respectively. Parameter values are listed in Appendix B. The general order of daily processes for the egg-YOY model is the same as the juvenile/adult model. The sub-model consists of egg, yolk-sac, and post-larval/YOY stages.

2.3.1 Population Dynamics

A batch (*b*) of eggs (all eggs laid by spawning adults on a given day) is followed through time and survival is modeled by using an exponential decay equation (Eq. EY.1). Daily M^{eggs} is drawn randomly from a uniform distribution with range 0.14-0.30 (Appendix B) developed from the literature (Supplemental Document Section 4). The day on which a batch of eggs hatch is determined using a hatch time (*h*) and temperature (*T*) relationship (Eq. EY.2) developed from Edsall (1970)(full details in Supplementary Document Section 5). The rate of development to hatching is dependent on daily temperature and the fraction of the development that occurs on a given day is calculated as *1/h*. Hatching occurs on day *d* according to Eq. EY.3. The number of yolk-sac larvae that hatch is derived from the number of surviving eggs reduced for hatching success (Eqs. EY.4 and EY.5). The hatching success versus temperature relationship was developed from Edsall (1970)(full details in Supplementary Document Section 6). Survival of yolk-sac larvae also follows the exponential decay equation and a multiplier is available to rescale *M* if desired (Eq. EY.5). The day on which complete yolk-sac absorption occurs (*d(y)*) is derived from the inverse of a days-to-yolk absorption and temperature relationship created from literature values (Eqs. EY.6 and EY.7)(full details in Supplementary Document Section 7). Multipliers are available to rescale *M* in the egg and yolksac stages (Eqs. EY.1 and EY.5).

288

289 *2.4 Post-Larvae/ YOY Population Dynamics*

290 *2.4.1 Initial Density-Dependent Mortality*

291 Population growth is limited by a simple density-dependent function. On the first day
292 that yolk-sac larvae become post-larvae (Eq. EY.8), the number is further reduced by a batch
293 carrying capacity (k_b) derived from a user-specified number of post-larvae per km^2 that a lake
294 can hold, the lake area (km^2) and the total number of batches (Eqs. EY.9 and EY.10)(full details
295 in Supplementary Document Section 8).

296

297 *2.4.2 Length Platoons*

298 The number of post-larvae in each batch is distributed into length platoons (L_p) on the
299 first day. The length bins are first created by using the minimum and maximum observed
300 lengths of post-larval Alewife (Eq. EY.11), density frequencies from a log-normal distribution
301 are generated using the mean of log-transformed length and standard deviation of log values (Eq.
302 EY.12), and then the number of post-larvae is assigned across length bins by randomly sampling
303 from a multinomial distribution parameterized with probability π (Eqs EY.13 and EY.14))(full
304 details in Supplementary Document Section 9).

305

306 *2.4.3 Population Dynamics*

307 A batch of post-larvae is followed through time and the decline in numbers is modeled
308 using the exponential decay model with a stage multiplier (Eq. EY.15) where M^{Post} is length-
309 dependent daily instantaneous natural mortality (Eq. EY.16). Natural mortality for fish $\leq$ 22 mm
310 total length (TL) is dependent on length and water temperature, whereas it is only length-

311 dependent for fish > 22 mm TL. These relationships were developed from and calibrated with
312 published literature values (full details in Supplementary Document Section 10).
313
314 *2.4.4 Growth in Lake*
315 The body length of platoon *p* on day *d* is calculated from body length at the start of day
316 *d-1* and the daily growth increment derived by using the Alewife bioenergetics model of Stewart
317 and Binkowski (1986) with improvements by Klumb et al. (2003). This model is based on an
318 energy balance equation, $\Delta B = C-(R+S+ER+U)$, where ΔB is the daily increase in body weight, C
319 is daily consumption, R is energy lost through metabolism, S is energy lost to specific dynamic
320 action, ER is energy lost in egestion, and U is energy lost in excretion. The definitions of
321 symbols and the equations governing the functional relationships are given in Tables 6 and 7,
322 respectively. Parameter values are listed in Appendix C. Daily consumption and standard
323 metabolism are the only temperature-dependent processes in the model.
324 In the growth sub-model, length of platoon *p* is first converted to weight using length-
325 weight equations depending on body length (Eq. BE.1). Daily consumption (joules• g^{-1} •d^{-1}) by
326 platoon *p* is then calculated following Eq. BE.2 where C_{max} is the maximum specific feeding rate
327 (g •g^{-1} •d^{-1}) dependent on size (Eq. BE.3), *EDP* is the prey energy density (joules g^{-1}; calculated
328 from prey specific energy densities for the average stomach contents of Alewife post-larvae in
329 Cohen (1976), *pr* is the proportion of maximum consumption dependent on body length and
330 abundance (Eqs. BE.4 and BE.5), and $f(T_d)$ is the temperature-dependence function for cold-
331 water species (Thornton and Lessem, 1978)(Eqs. BE.6- BE.12). The *pr* and length L_p
332 relationships (Eq. BE.4) were developed and calibrated to obtain length ranges described in
333 several published studies and unpublished field data from Massachusetts and Rhode Island

334 sampling programs that occurred in rivers, lakes, estuaries and ocean waters (full details in
335 Supplementary Document Section11) . A relationship between slope of the *pr* relationship and
336 number of young on a given day was further developed to simulate density-dependent growth
337 (Eq. BE.5)(full details in Supplementary Document Section12). Regional growth multipliers are
338 included and the estuary region multiplier (Ω_2) is set to 1.40 to match size data of young-of-the-
339 year Alewife from Narragansett Bay, Rhode Island.

340 Respiration is calculated through a standard metabolism-body weight relationship,
341 activity multiplier and a temperature dependence function (Eq. BE.13) where R_p is specific rate
342 of respiration (joules• g^{-1} •d^{-1}) for platoon *p*, *ACT* is a length-dependent activity multiplier to
343 obtain active metabolism (Eqs. BE.14 and BE.15), $f(T_d)$ is the temperature dependence function
344 (Eq. BE 16), and *OC* is the oxycalorific coefficient used to convert grams to joule equivalents.
345 Egestion rate (ER; joules• g^{-1} •d^{-1}) is calculated assuming a constant fraction of consumption (Eq.
346 BE.17). Excretion (U; joules• g^{-1} •d^{-1}) is derived assuming a constant fraction of assimilated
347 energy (Eq. BE.18), and specific dynamic action (SDA) is calculated assuming a constant
348 fraction of assimilated energy lost (Eq. BE.19).

349 Daily body weight increase is derived via Eqs BE.20- BE.22. The energy density (ED;
350 joules• g^{-1}) of Alewife to convert joules to grams is calculated from seasonal relationships
351 between ED and body length (Eq. BE.22). To obtain the daily change in length, weight is
352 converted to length by using length-weight equations (Eq. BE.23).

353 Because the observed daily lake temperature may not match the temperature actually
354 selected by the young Alewives, an optimal temperature-length relationship is used to replace the
355 observed lake temperature (usually measured at the surface) when it exceeds the optimal
356 temperature (Eq. BE.24). This assumes YOY are actively seeking optimal temperatures.

357

358 *2.4.5 Emigration from Lake*

359 Based on results of Gahagan et al. (2010), movement of YOY from the lake is dependent
360 on body size, temperature and rainfall. The first day of emigration can begin when the body
361 length of any platoon exceeds the user-specified migration size. The end day of emigration is
362 randomly picked to occur between day 304 and day 334. The number of fish that emigrate at the
363 beginning of day *d* is calculated according to Eq. EY.17 in Table 5 and the fraction emigrating is
364 determined using temperature and rainfall relationships developed from raw data of Gahagan et
365 al. (2010) (Eqs. EY.18-EY.20)(full details in Supplementary Document Section 13). Number of
366 fish remaining in the lake is determined by Eq. EY.21.

367

368 *2.4.6 Movement from River to Ocean*

369 The amount of time spent in the river (*rdur*) and estuary (*edur*) is determined from
370 swimming speed (V; cm s^{-1}) of YOY and system length (Eqs. EY.23- EY.24). Any remaining
371 YOY in the estuary are moved to the ocean region on January 1 of the following year and the
372 YOY become immature age 1 fish. Numbers are split between sexes using a constant proportion
373 of females ($p♀$).

374

375 *2.4.7 Mortality in River, Estuary and Ocean*

376 Mortality is calculated following Eq. EY.16.

377

378 *2.4.8 Growth in River, Estuary and Ocean*

379 Daily growth in the river, estuary and ocean is calculated by using the bioenergetics sub-
380 model, the daily temperature from each region and the optimal temperature-body size
381 relationship.
382
383 2.5. *Global Sensitivity Analysis*
384 The sensitivities of model outputs to input parameters were explored by using the method
385 of Morris (1991). This global sensitivity method was used to identify parameters with a range of
386 negligible to strong impacts. In addition, the Morris method identifies linear and nonlinear
387 effects. The Morris method consists of several randomized one-at-a-time experiments in which
388 the effect of a parameter on the model output is assessed while keeping the other parameters
389 constant (van Houwelingen et al., 2011). The first step is to randomly draw a set of starting
390 values within defined ranges of possible values for all input parameters, running the model using
391 these initial starting values, and saving the model output. The second step changes the value of
392 one parameter by a random interval (all other parameter values are those from the last run) and
393 the model output is then compared the previous run. For comparison, the elementary effect of the
394 i^{th} (*EE*) input parameter is calculated by
395
396 $$EE_i(x^t) = \left(y(x^t) - y(x^{t-1})\right)/\pm\Delta_i$$
397
398 where *y* is the model output variable of interest, *t* is the current run and Δ_i is the random change
399 interval based on p=4 (See van Houwelingen et al., 2011 for more details). The process is
400 repeated for the remaining variables. The entire procedure is repeated *r* times (*r*=10 in this
401 paper), each time with a different set of initial starting values. The total number of runs needed

for the analysis are $r(n+1)$ where n is the number of parameters. The mean (μ*), absolute mean (μ) and standard deviation (σ) are then calculated for the i^{th} input parameter by

$$\mu_i^* = \sum_{j=1}^{r} EE_{i,j}/r$$
$$\mu_i = \sum_{j=1}^{r} |EE_{i,j}|/r$$
$$\sigma_i = \sqrt{\sum_{j=1}^{r} \left(EE_{i,j} - \mu_i^*\right)^2/r}$$

The interpretation of a parameter's effect is based on the coupled μ and σ values. Low μ and σ values imply a parameter has a low impact on the model output, high μ and low σ imply a parameter has high linear impacts on the model, low μ and high σ values imply a parameter has high nonlinear impacts on the model, and high μ and high σ values imply a parameter has high nonlinear impacts on the model and/or strong interactions with other parameters (Loubiere et al., 2016). We explored the sensitivity of only seventy-five parameters because valid minimum-maximum ranges could not be derived for some given lack of literature (e.g., the temperature function parameters used in the bioenergetics model) or changes in individual parameters could not be examined independently (e.g., the polynomial relationship parameters between hatching success and temperature) without producing non-sensical values. The list of parameters with corresponding ranges for the uniform distributions are provided in Appendix Table D.1. Ranges were derived mainly from literature, but when lacking, ranges were also derived from standard error estimates (±2 SE) of parameters (e.g., male and female von Bertalanffy growth) or from within a biologically-realistic range based on our best judgement (e.g., $p♀$).

For each run, the model was initialized with an equilibrium population of juveniles and adults (full details in Supplementary Document Section 14). The model was then run for 30

424 years (duration population reaches equilibrium with new parameters) using regional temperature
425 and rainfall data from 1962-1992 (obtained from various data sources or developed from air
426 temperature for the region of Narragansett Bay through Southern Massachusetts (full details in
427 Supplementary Document Sections 15-17)) . The last year's derived values of run size, mean
428 length of adults in the river, sex ratio on the run, egg abundance, YOY cumulative river
429 abundance, and age-1 mean length on January 1 were recorded and used to examine input
430 parameter sensitivities.
431
432 2.6. *Model Validation*
433 Confidence in the performance of the model may be evaluated in terms of its ability as a
434 predictive tool (Balci, 1998). To validate model results, we compared predicted dates of run
435 starts, sex-specific mean ages on the run, ranges of days of first hatching and mean total length
436 of age1 fish in spring to published and unpublished field observations not used in the calibration
437 of the model. The model was run 50 times with only baseline natural mortality, and temperature
438 and rainfall data from 1962-2016, and the mean and 95th percentiles of the outputs were used for
439 comparison.
440
441 2.7. *Exploration of Hypotheses of Population Changes*
442 To demonstrate the model's potential to explore factors that may have caused historical
443 changes in Alewife population characteristics, we investigated three spatial mortality hypotheses:
444 historical responses were caused by 1) in-river harvest only, 2) in-river striped bass predation
445 and harvest, and 3) ocean by-catch in the Atlantic herring fishery and in-river harvest. We expect
446 population responses to differ among these hypotheses because most of the population is

447 vulnerable to incidental capture in the ocean region, whereas only immigrating, mature adults are
448 vulnerable to predation by Striped Bass in the river region. Time series of mortality rates
449 attributed to each component were created from existing data. In-river exploitation rates from
450 the Monument River (Nelson et al., 2011) were used to represent the fraction of adults harvested
451 in the river system. No harvest was assumed after 2005 because a moratorium in Massachusetts
452 has been in place. Since Striped Bass prey on migrating river herring (e.g., Davis et al., 2012),
453 predation mortality rates were associated with the river region and represented the daily fraction
454 of the adults eaten in the river system. Values were derived from data on Striped Bass
455 abundance and estimates of instantaneous total mortality from a statistical escapement-at-age
456 model. Bycatch mortality rates, representing the fraction of ocean population harvested by
457 incidental capture, were similarly derived by using New England Atlantic herring fishery
458 landings (see section 18 of Supplementary Document for full details). For each scenario, the
459 model was run 75 times (runtime: ~ 65 hours with Intel i7-6700 CPU @ 3.40 GHz) for 55 years
460 with water surface temperature and rainfall for years 1962-2016 (trends related to climate change
461 are evident in the time series; Supplemental Document Section 15-17). The model was initialized
462 at the start of each run with the equilibrium population of juveniles and adults described above.
463
464 **3. Results**
465 *3.1 Global Sensitivity*
466 Results of the sensitivity analysis indicated that the model is highly non-linear and there
467 are strong interactions among parameters (Figure 3). The top twenty parameters based on μ*
468 that play a significant role in the magnitude of fluctuations in model output are shown in Table 8.
469 The run size and mean length of adults on the run are sensitive primarily to changes in

parameters from the bioenergetics sub-model, juvenile/adult mortality equations, post-larvae/YOY mortality and adult maturity (Table 8). The run sex ratio is most sensitive to changes in the $p♀$ (proportion used to split YOY into sexes), and maturity and bioenergetics model parameters (Table 8). Egg abundance is most sensitive to parameter changes in the bioenergetics model, juvenile/adult mortality equation and post-larvae/YOY mortality equation. Abundance of YOY is very sensitive to changes in lake carrying capacity, post-larvae/YOY mortality and bioenergetics model parameters (Table 8). The mean length of age-1 fish on January 1 is sensitive primarily to changes in the bioenergetics model parameters (Table 8).

3.2 Model Validation

Figure 4 shows the model output and data from published and unpublished field data. Model predictions of run starts matched well ranges of run starts observed in the Parker River, Massachusetts during 1972-1978 (Cole et al., 1976; Cole et al., 1978), in the Annaquatucket River, Rhode Island during 1971 and 1972 (Richkus, 1974) and in multiple Massachusetts systems monitored in 2014 (Rosset et al., 2017)(Figure 4A). The predicted mean age of female and male Alewife during 1972-1978 agreed well with observed mean ages in the Parker River (Cole et al., 1976; Cole et al., 1978) (Figure 4B). The range of model predictions of the first day of hatching was similar to those observed in field studies (Yako, 1998; Iafrate and Oliviera, 2008; Devine, 2018) (Figure 4C). The model predicted well the mean lengths and 95% length percentiles of age-1 Alewife compared to length data recorded in the MA DMF trawl survey and Atlantic herring bycatch sampling during 2012-2016 (Figure 4D). Overall, the model produced realistic trends and ranges of population characteristics observed historically.

493 *3.3 Exploration of Hypotheses of Population Changes*

494 Generally, harvest mortality has changed in an inverse relationship to recently dominant
495 striped bass predation and bycatch mortality (Figure 5). All hypotheses produced similar trends
496 in run size, mean length and mean age through 1990, but changes in population characteristics
497 were larger under hypotheses 2 (in-river harvest plus Striped Bass mortality) and 3 (in-river
498 harvest plus bycatch mortality) because of higher combined mortalities (Figure 6). The largest
499 decline in run size occurred when bycatch mortality was present, but the simulated decline began
500 much earlier (1991) than was observed in Monument River (Figure 6). Under hypotheses 2 and
501 3, the model simulated declines in mean total length starting in 1991, which was close to
502 observed start years (1989-1990), but similar magnitudes in body size reduction (20-30 mm TL)
503 as observed in the Monument River were not reproduced (Figure 6). The model under
504 hypotheses 2 and 3 predicted declines in mean age of females, and the trends and magnitudes
505 under each hypothesis partially matched the trends and magnitudes observed in the Monument
506 River (Figure 6).

507

508 **4. Discussion**

509 We have developed, calibrated and validated a full life-cycle model for Alewife for
510 evaluating hypotheses of potential causal factors affecting population dynamics. Key features of
511 the model are that it (1) is structured sufficiently to provide realistic dynamics without being
512 individually-based; (2) includes the full life cycle; (3) includes a realistic growth model for YOY
513 Alewife; (4) includes environmental drivers that are known to influence growth, survival and
514 migration processes during the first year of life; (5) has a generalized spatial structure and (6)
515 incorporates exploitation and predation. This model should improve Alewife restoration efforts

516 by providing a tool to better understand factors influencing demographic trends and the
517 consequences of potential management actions or environmental change.
518 The model is the first of its kind for Alewife and is an advancement towards
519 understanding the impact of exogeneous factors on the population dynamics of Alewife; however
520 it is generic and is not a complete representation of all processes that may affect Alewife
521 population dynamics. For example, there are currently no links between prey abundance and
522 growth of juvenile/adults and YOY Alewife or coupling between adult ocean migration and
523 environmental variables. In some aspects, we had to develop methods that would simulate trends
524 in population characteristics similar to those observed in the field without understanding
525 underlying processes. In other aspects, processes had to be simplified or left out, and many
526 parameters were assumed constant because of lack of data. As data become available, additional
527 details of underlying dynamics may be easily added given the flexible sub-model structures and
528 coding in the R language.
529 We have demonstrated the power of the model to explore population responses by
530 simulating three hypotheses concerning spatial exploitation and predation. Under these simple
531 hypotheses, the model did predict similar trends in population characteristics as those observed
532 historically in southern New England runs, but the timing and/or magnitudes of change were not
533 always replicated. This is not surprising given the limited hypotheses examined. These results
534 stress the fact that the reasons for the dramatic changes observed in the field are likely more
535 complex. To that end, the model has the ability to evaluate complex hypotheses if sufficient data
536 are available representing the specific aspects of growth and survival in a system. The population
537 consequences of management actions pertaining to juvenile/adult Alewife and its predators can
538 be simulated through the link with mortality. The effects of climate change, expected to be a

539 major stressor on Alewife populations (Hare et al., 2016; Lynch et al., 2015), on population
540 responses could be examined because water temperature is directly coupled to the start of adult
541 migration, spawning initiation, egg hatching rate, yolk-sac absorption, growth, mortality and
542 emigration of post-larval/YOY stages, while rainfall is linked to emigration of YOY.
543 For instance, if forecasts of water temperatures are available, the consequences of temperature-
544 related changes in reproductive processes (e.g., earlier spawning times and/or hatching times) on
545 dynamics that can impact future recruitment (e.g., Lowerre-Barbieri et al., 1998) could be
546 explored. Similarly, if forecasts of rainfall are available, the consequences of potential changes
547 in YOY emigration timing as rainfall changes on similar dynamics and resulting processes could
548 be examined.
549 The sensitivity analysis showed that the most influential parameters in the model are
550 those associated with the post-larvae/YOY bioenergetics growth model and the
551 juvenile/adult/YOY mortality relationships. It is important that those parameters have a low
552 degree of uncertainty associated with them to allow for accurate prediction. Unfortunately,
553 measures of uncertainty are not available for most parameters used in the model because many
554 authors did not include statistics associated with model parameters (e.g., Stewart et al., 1983),
555 although some did include information on model fit (e.g., R^2; Pepin, 1991) (Appendix D). For
556 parameters with measures of uncertainty (e.g., coefficients of variation), precision appears
557 reasonably high (CVs <20%) in most cases. The lack of measures of uncertainty for many
558 parameters does not mean the model predictions will be inaccurate. Stewart et al. (1983) showed
559 the bioenergetics model produces realistic growth predictions, and will likely do so under a wide
560 range of scenarios, because most parameters were determined through laboratory studies. In
561 addition, the *pr* relationships and Ω_2 were calibrated to field observations of post-larvae and

562 YOY sizes, and predictions were validated against data not used in the calibration (Figure 4D).
563 Similarly, we are confident that the mortality relationships will also produce realistic values
564 because they were calibrated to literature-based observations of survival.

565 There are many biotic and environmental drivers affecting productivity of young Alewife
566 while in freshwater system (Kosa and Mather 2001; Yako et al., 2002). Based on the sensitivity
567 analysis results, the model outputs reflecting system productivity (e.g., YOY abundance) were
568 most affected by changes in parameters of the growth and mortality components (including the
569 carrying capacity parameter). Although we developed components of the relationship from
570 limited data, in reality, they are simple and generic. It is unlikely that more detailed lake-specific
571 predictions of production could be made unless data on important abiotic and environmental
572 drivers are known for each system. Ultimately, lake-specific differences in drivers will result in
573 varying levels of production that will determine individual population resilience to
574 anthropogenic and environmental stressors.

575 A benefit of creating an empirically-based life cycle model is learning where gaps in our
576 current knowledge of biological processes and population dynamics are. More detailed
577 information on Alewife population dynamics are needed at all life stages. Some areas of
578 necessity include Alewife-specific egg and yolk-sac mortality rates, relationships between YOY
579 growth and prey, and environmental and physiological influences that affect adult immigration
580 and YOY emigration. Some of the biggest gaps in our knowledge pertain to the times YOY and
581 adults spend in an estuary and ocean. For YOY, there is some general information on growth and
582 broad habitat use between freshwater and estuarine environments (Turner and Limburg 2012;
583 Turner and Limburg 2016). However, no information exists on the duration spent in an estuary,
584 prey species eaten in estuaries and the ocean, spatial distribution, mortality and movement

585 patterns that would help improve our understanding of YOY dynamics and allow us to enter
586 more detail into the model. For adults, general migration patterns are assumed (north into the
587 Gulf of Maine after spawning, south to waters south of Cape Cod in the winter (Munroe, 2002)),
588 but details on movements and spatial distribution for individual stocks or regional groups are
589 needed to help resolve a multitude of fishery and climate change impacts (ASMFC 2012;
590 Hasselman et al. 2016; Hare et al. 2016; Lynch et al. 2015; Palkovacs et al. 2013). This is
591 particularly important since migration routes will influence the exposure of Alewife to fisheries
592 impacts over space and time (Bethoney et al., 2017).

593 Over the past ten years, Alewife have been the focus of two Endangered Species Act
594 Listing Determinations, a Benchmark Stock Assessment, and Stock Assessment update. The
595 resounding conclusion of all of these examinations is that status determination, management and
596 recovery of this species is hindered by a lack of data and tools. This model represents a
597 significant step forward in our ability to understand Alewife population dynamics and should
598 improve restoration efforts. Still, until deeper understanding of underlying processes and long-
599 term time series of environmental and biological measures are available, it may be impossible to
600 identify primary factors responsible for the historical changes in Alewife populations. New
601 technologies, including bio-logging (e.g., Dean et al., 2017), and additional data collected across
602 the life cycle will be key to closing the data gaps and making Alewife assessment and
603 management a more data-rich effort.

604

Acknowledgements

Funding for this project was provided, in part, by the Atlantic States Marine Fisheries Commission and by Sportfish Restoration Grant F-57R. We thank the following individuals and institutions for providing Alewife data: Matthew Devine of the University of Massachusetts-Amherst, John Sheppard, Bradley Schondelmeier and the Age and Growth staff of Massachusetts Division of Marine Fisheries, Phil Edwards of the Rhode Island Department of Fish and Wildlife, Kurt Gottschall of the Connecticut Department of Environmental Protection and the University of Rhode Island Graduate School of Oceanography. All members of the NOAA funded Linking Lifestages project provided helpful comments during the initial stages of model creation. We also thank two anonymous reviewers for helpful comments that improved the manuscript. The entire model code and data used in this study are available upon request from the senior author.

References

Archambault, B., Rivot, E., Savina, M., Le Pape, O., 2018. Using a spatially structured life cycle model to assess the influence of multiple stressors on an exploited coastal-nursery-dependent population. Estuar. Coast. Shelf Sci. 201: 95-104. https://doi.org/10.1016/j.ecss.2015.12.009

ASMFC (Atlantic States. Marine Fisheries Commission), 2012. River herring benchmark stock assessment Volume I. Stock Assessment Report 12-02 of the Atlantic States Marine Fisheries Commission, Washington, DC.

ASMFC (Atlantic States. Marine Fisheries Commission), 2017. River Herring Stock Assessment Update, Volume I: Coastwide Summary. 172 p. Arlington, VA.

Balci, O., 1998. Verification, Validation and Testing. *In*: Handbook of Simulation: Principles, Methodology, Advances, Applications and Practice, J. Banks (ed.), John Wiley and Sons, Inc. New York, New York, p.335-393.

Bethoney, N. D., Schondelmeier, B. P., Kneebone, J., Hoffman, W. S., 2017. Bridges to best management: effects of a voluntary bycatch avoidance program in a mid-water trawl fishery. Mar. Pol. 83: 172-178. https://doi.org/10.1016/j.marpol.2017.06.003.

Burbidge, R. G., 1974. Distribution, growth selective feeding, and energy transformations of young-of-the-year blueback herring, *Alosa aestivalis* (Mitchill), in the James River, Virginia. Trans. Am. Fish. Soc.103: 297-311. https://doi.org/10.1577/1548-8659(1974)103<297:DGSFAE>2.0.CO;2

Cole, C. F., Libey, G. S., Huber, M. E., Jimenez, D., 1976. Optimal alewife run management, Parker River, Massachusetts. Final Report to U.S. Department of Commerce, National Oceanic and Atmospheric Administration, National Marine Fisheries Service. Project AFC-12. 37 p.

Cole, C. F., Essig, R., Sarnelle, O., 1978. Biological investigation of the alewife population, Parker River, MA. Anadromous Fish Act Yearly Report to U.S. Department of Commerce, National Oceanic and Atmospheric Administration, National Marine Fisheries Service. Project AFC-16-2. 16.p.

Cournane, J. M., Kritzer, J. P., Correia, S. J., 2013. Spatial and temporal patterns of anadromous alosine bycatch. Fisheries Research 141: 88-94. https://doi.org/10.1016/j.fishres.2012.08.001

Dalton, C. M., Ellis, D., Post, D. M. 2009. The impact of double-creasted cormorant (*Phalacrocorax auritus*) predation on anadromous alewife (*Alosa pseudoharengus*) in south-central Connecticut, USA. Can. J. Fish. Aquat. Sci. 66: 177-186. https://doi.org/10.1139/F08-198

664 Davis, J. P., Schultz, E. T. 2009., Temporal shifts in demography and life history of an
665 anadromous alewife population In Connecticut. Mar. Coast. Fish. Dyn. Manage and
666 Ecosystem Science. 1: 90:106. https://doi.org/10.1577/C08-003.1

667 Davis, J. P., Schultz, E. T., Vokoun, J. C., 2012. Striped Bass consumption of Blueback herring
668 during vernal riverine migrations: does relaxing harvest restrictions on a predator help
669 conserve a prey species of concern? Marine and Coastal Fisheries Dynamics,
670 Management and Ecosystem Science 4: 239-251.
671 https://doi.org/10.1080/19425120.2012.675972.

672 Dean, M. J., Hoffmans, W. S., Zemeckis, D. R., Armstrong, M. P., 2017. Fine-scale diel and
673 gender-based patterns in behaviour of Atlantic cod (Gadus morhua) on a spawning
674 ground in the Western Gulf of Maine. ICES J. Mar. Sci. 71: 1474-1489.
675 https://doi.org/10.1093/icesjms/fsu040.
676
677 Diaz, B. S., Frisk, M. G., Jordaan, A., 2019. Opening the tap: increasing riverine connectivity
678 strengthens marine food web pathways, PLoS ONE 14(5):e0217008.
679 https://doi.org/10.1371/journal. pone.0217008.
680
681 Edsall, T. A., 1970. The effect of temperature on the rate of development and survival of alewife
682 eggs and larvae. Trans. Am. Fish. Soc. 99: 376-380. https://doi.org/10.1577/1548-
683 8659(1970)99<376:TEOTOT>2.0.CO;2
684
685 Ellis, D., Vokoun, J. C., 2009. Earlier spring warming of coastal streams and implications for
686 alewife migration timing. N. Am. J. Fish. Manage. 29: 1584-1589.
687 https://doi.org/10.1577/M08-181.1
688
689 Fay, C.W., Neves, R. J., Pardue, G. B., 1983. Species profiles: life histories and environmental
690 requirements of coastal fishes and invertebrates (Mid-Atlantic) - alewife/blueback
691 herring. U. S. Fish and Wildlife Service, Division of Biological Services,
692 FWS/OBS.82/11.9. U. S. Army Corps of Engineers TR EL-82-04. 25 p.
693
694 Gahagan, B. I., Gherard, K. E., Schultz, E. T., 2010. Environmental and endogeneous factors
695 influencing emigration in juvenile anadromous alewives. Trans. Am. Fish. Soc. 139:
696 1069-1082. https://doi.org/10.1577/T09-128.1
697
698 Ganias, K., Divino, J. N., Gherard, K. E., Davis, J. P., Mouchlianitis, F., Schultz, E. T., 2015. A
699 reappraisal of reproduction in anadromous alewives: determinate versus indeterminate
700 fecundity, batch size, and batch number. Trans. Am. Fish. Soc. 144: 1143-1158.
701 https://doi.org/10.1080/00028487.2015.1073620
702
703 Gibson, A. J. F., Myers, R. A., 2003. A statistical, age-structured, life-history-based stock
704 assessment model for anadromous *Alosa*. Pages 275-283 *in* Limburg, K. E., Waldman, J.
705 R., editors. Biodiversity, status, and conservation of the world's shads. American
706 Fisheries Society Symposium 35, Bethesda, Maryland.
707

708 Goodyear, C. P., 1989. LSIM – a length-based fish population simulation model. NOAA Tech.
709 Memo. NMFS-SEFC 219. 53 p.
710
711 Goodyear, C. P., 2002. Negative implications of large minimum size regulations on future mean
712 size at age: an evaluation using simulated striped bass data. Am. Fish. Soc. Sym. 30: 217-
713 229.
714
715 Hall, C. J., Jordaan, A., M. G. Frisk., 2012. Centuries of anadromous forage fish loss:
716 consequences for ecosystem connectivity and productivity. Bioscience 62 (8): 723-731.
717 https://doi.org/10.1525/bio.2012.62.8.5
718
719 Hare, J.A., Morrison, W. E., Nelson M. W., Stachura, M. M., Teeters, E. J., Griffis, R. B.,
720 Alexander, M. A., Scott, J. D., Alade, L., Bell, R. J., Chute, A. S., Curti, K. L., Curtis,
721 T.H.,Kircheis, D., Kocik, J. F., Lucey, S. M., McCandless, C. T., Mike, L. M.,
722 Richardson, D. E., Robillard, E., Walsh, H. J., McManus, M. C., Marancik, K. E.,
723 Griswold, C. A., 2016. A vulnerability assessment of fish and invertebrates to climate
724 change on the Northeast U. S. Continental Shelf. PLoS ONE 11(2): e0146756. .
725 https://doi.org/10.1371/journal.pone.0146756.
726
727 Hasselman, D. J., Anderson, E. C., Argo, E. E., Bethoney, N. D., Gephard, S. R., Post, D. M.,
728 Schondelmeier, Schultz, T. F., Willis, T. V., Palkovacs, E. P., 2016. Genetic stock
729 composition of marine bycatch reveals disproportional impacts on depleted river herring
730 genetic stocks. Can. J. Fish. Aquat. Sci. 73: 951-963. https://doi.org/10.1139/cjfas-2015-
731 0402.
732
733 Iafrate, J., Oliveira, K., 2008. Factors affecting migration patterns of juvenile river herring in a
734 coastal Massachusetts stream. Environ. Biol. Fish. 81:101-110.
735 https://doi.org/10.1007/s10641-006-9178-1.
736
737 Kane, J., 2011. Multiyear variability of phytoplankton abundance in the Gulf of Maine. ICES J.
738 Mar. Sci. 68: 1833-1841. https://doi.org/10.1093/icesjms/fsr122.
739
740 Kissel, G. W., 1974. Spawning of the anadromous alewife, *Alosa pseudoharengus*, in Bride
741 Lake, Connecticut. Trans. Am. Fish. Soc. 103: 312-317. https://doi.org/10.1577/1548-
742 8659(1974)103<312:SOTAAA>2.0.CO;2.
743
744 Kitchell, J. F. Stewart, D. J., Weininger, D., 1977. Applications of a bioenergetics model to
745 yellow perch (*Perca flavescens*) and walleye (*Stizostedion vitreum vitreum*). J. Fish. Res.
746 Board Can. 34: 1922-1935. https://doi.org/10.1139/f77-258.
747
748 Klumb, R. A., Rudstam, L. G., Mills, E. L., 2003. Comparison of alewife young-of-the-year and
749 adult respiration and swimming speed bioenergetics model parameters: implications of
750 extrapolation. Trans. Am. Fish. Soc. 132: 1089-1103. https://doi.org/10.1577/T03-038.
751

752 Loesch, J. G., 1987. Overview of life history aspects of anadromous alewife and blueback
753 herring in freshwater habitats. In: M. J. Dadswell et al., eds., Common Strategies of
754 Anadromous and Catadromous Fishes. Am. Fish. Soc. Symp. 1: 89-103.
755
756 Lorenzen, K., 1996. The relationship between body weight and natural mortality in juvenile and
757 adult fish: a comparison of natural ecosystems and aquaculture. J. Fish Biol. 49: 627–
758 642. https://doi.org/10.1111/j.1095-8649.1996.tb00060.x.
759
760 Loubiere, P., Jourdan, A., Siarry, P., Chelouah, R., 2016. A sensitivity analysis method for
761 driving the Artificial Bee Colony algorithm's search process. Appl. Soft. Comput.
762 41:515-531. https://doi.org/10.1016/j.asoc.2015.12.044.
763
764 Lowerre-Barbieri, S. K., Lowerre, J. M., Barbieri, L. R. 1998. Multiple spawning and the
765 dynamics of fish populations from an individual-based simulation model. Can. J. Fish.
766 Aquat. Sci. 55: 2244-2254.
767
768 Lynch, P. D., Nye, J. A., Hare, J. A., Stock, C. A., Alexander, M. A., Scott, J. D., Curti, K. L.,
769 Drew, K., 2015. Projected ocean warning creates a conservation challenge for river
770 herring populations. ICES J. Mar. Sci. 72: 374-387.
771 https://doi.org/10.1093/icesjms/fsu134.
772
773 Maki, K. L., Hoenig, J. M., Olney, J. E., 2001. Estimating proportion mature at age when
774 immature fish are unavailable for study, with applications to American shad in the York
775 River, Virginia. N. Am. J. Fish. Manage. 21: 703-716. https://doi.org/10.1577/1548-
776 8675(2001)021<0703:EPMAAW>2.0.CO;2.
777
778 Morris, M. D., 1991. Factorial sampling plans for preliminary computational experiments.
779 Technometrics 33: 161-174. http://dx.doi.org/10.1080/00401706.1991.10484804.
780
781 Mullen, D.M., Fay, C. W., Moring, J. R., 1986. Alewife/Blueback Herring. Species Profiles: Life
782 Histories and Environmental Requirements of Coastal Fishes and Invertebrates (North
783 Atlantic series) USDI Fish and Wildlife Service. Biological Report 82(11.58). 22 pp.
784
785 Munroe, T. A., 2002. Herrings. Family Clupeidae: Alewife. *In*: Collette, B. B., Klein-MacPhee,
786 G. (eds.), Bigelow and Schroeder's Fishes of the Gulf of Maine, 3rd edition. Smithsonian
787 Institution Press, Washington, DC. pp. 118-125.
788
789 Nelson, G. A., Brady, P. D., Sheppard, J. J., Armstrong, M. P., 2011. An assessment of river
790 herring stocks in Massachusetts. Massachusetts Division of Marine Fisheries Tech. Rep.
791 TR-46. 81 p. https://www.mass.gov/files/documents/2016/08/wi/tr-46.pdf.
792
793 Nye, J. A., Link, J. S., Hare, J. A., Overholtz, W. J., 2009. Changing spatial distribution of fish
794 stocks in relation to climate and population size on the Northeast United States
795 continental shelf. Mar. Ecol. Prog. Ser. 393: 111-129.
796 https://doi.org/10.3354/meps08220.
797

798 Palkovacs, E. P., Hasselman, D. J., Argo, E. E., Gephaerd, S. R., Limburg, K. E., Post, . M.m
799 Schultz, T. F., Willis, T. V., 2013. Combining genetic and demographic information to
800 prioritize conservation efforts for anadromous alewife and blueback herring. Evol. Appl.
801 7: 212-216. https://doi.org/10.1111/eva.12111.
802
803 Pauly, D., 1984. Length-converted catch curves. A powerful tool for fisheries research in the
804 tropics (Part III). ICLARM Fishbyte 2(1): 17-19.
805
806 Pepin, P., 1991. Effect of temperature and size on development, mortality, and survival rates of
807 the pelagic early life history stages of marine fish. Can. J. Fish. Aquat. Sci. 48: 503-518.
808 https://doi.org/10.1139/f91-065.
809
810 Pershing, A. J., Greene, C. H., Jossi, J. W., O'Brien, L, Brodziak, J. K. T., Baily, B.A., 2005.
811 Interdecadal variability in the Gulf of Maine zooplankton community, with potential
812 impacts on fish recruitment. ICES J. Mar. SCi. 62:1511-1523.
813 https://doi.org/10.1016/j.icesjms.2005.04.025.
814
815 Quinn, T. J., Deriso, R. B., 1999. Quantitative fish dynamics. Oxford University Press. 542
816 pages.
817
818 R Development Core Team. 2016. R: A language and environment for statistical computing. R
819 Foundation for Statistical Computing, Vienna, Austria. ISBN 3-900051-07-0,
820 http://www.R-project.org/.
821
822 Richkus, W. A., 1974. Factors influencing the seasonal and daily patterns of Alewife (Alosa
823 pseudoharengus) migration in a Rhode Island river. J. Fish. Res Boad Can. 31:1485-
824 1497. https://doi.org/10.1139/f74-178.
825
826 Rosset, J., Roy, A. H., Gahagan, B. I., Whiteley, A. R., Armstrong, M. P., Sheppard, J. J.,
827 Jordaan, A., 2017. Temporal patterns of migration and spawning of river herring in
828 coastal Massachusetts. Trans. Am. Fish. Soc 146: 1101-1114.
829 https://doi.org/10.1080/00028487.2017.1341851.
830
831 Savoy, T, Crecco, V., 1995. Factors affecting the recent declined of blueback and American shad
832 in the Connecticut River. A report to the Atlantic States Marine Fisheries Commission,
833 Washington, DC.
834
835 Schmidt, R. E., Jessop, B. M., Hightower, J. E., 2003. Status of river herring stocks in large
836 rivers. In: Limburg, K. E., Waldman, J. R., editors, Biodiversity, Status and Conservation
837 of the World's Shads. Am. Fish. Soc. Symp. 35:171-182.
838
839 Sheppard, J. J., Bednarski, M. S., 2015. Utility of single-channel electronic resistivity counters
840 for monitoring river herring populations. N. Am. J. Fish. Manage. 35: 1144-1151.
841 https://doi.org/10.1080/02755947.2015.1084407.
842

Stewart, D. J., Binkowski, F. P., 1986. Dynamics of consumption and food conversion by Lake Michigan alewives: an energetics-modeling synthesis. Trans. Am. Fish. Soc. 115: 643-661. https://doi.org/10.1577/1548-8659(1986)115<643:DOCAFC>2.0.CO;2.

Stewart, D. J., Kitchell, J. F., Rottiers, D. V., Edsall, T. A., 1983. An energetics model for lake trout, *Salvelinus namaycush*: application to the Lake Michigan population. Can. J. Fish. Aquat. Sci. 40: 681-698. https://doi.org/10.1139/f83-091.

Tommasi, D., Nye, J., Stock, C., Hare, J. A., Alexander, M., Drew, K., 2015. Effect of environmental condition on juvenile recruitment of alewife (*Alosa pseudoharengus*) and blueback herring (*Alosa aestivalis*) in freshwater: a coastwide perspective. Can. J. Fish. Aquat Sci. 72:1037-1047. https://doi.org/10.1139/cjfas-2014-0259.

Turner, S. M., Limburg, K. E.,2012. Comparison of juvenile alewife growth and movement in a large and a small watershed. Mar. Coast. Fish: Dyn. Manage. Eco. Sci. 4: 337-345. https://doi.org/10.1080/19425120.2012.675974.

Turner, S. M., Limburg, K. E., 2016. Juvenile river herring habitat use and marine emigration trends: comparing populations. Oecologia 180: 77-89. https://doi.org/10.1007%2Fs00442-015-3443-y.

Van Houwelingen, H. C., Boshuizen, H.C, Capannesi, M., 2011. Sensitivity analysis of state-transition models: how to deal with a large number of inputs. Comput. Biol. Med. 41:838-842. https://doi.org/10.1016/j.compbiomed.2011.07.001.

Walter s, A. W., Barnes, R. T., Post, D. M., 2009. Anadromous alewives (*Alosa pseudoharengus*) contribute marine-derived nutrients to coastal stream food webs. Can. J . Fish. Aquat. Sci.66: 439-448. https://doi.org/10.1139/F09-008.

Watermeyer, K. E., Jarre, A., Shannon, L. J., Mulumba, P. Botha, J., 2018. A frame-based modeling approach to understanding changes in the distribution and abundance of sardine and anchovy in the southern Benguela. Ecol. Model. 371: 1-17. https://doi.org/10.1016/j.ecolmodel.2017.12.017.

Yako, L. A., M. E. Mather, and F. Juanes., 2002. Mechanisms for migration of anadromous herring: an ecological basis for effective conversation. Ecol. Appl. 12: 521-534. https://doi.org/10.1890/1051-0761(2002)012[0521:MFMOAH]2.0.CO;2.

Zueg, S. C., Bergman, P. S., Cavallo, B. J., Jones, K. S., 2012. Application of a life cycle simulation model to evaluate impacts of water management and conservation actions on an endangered population of Chinook salmon. Environ. Model. Assess. 17: 455-467. https://doi.org/10.1007/s10666-012-9306-6.

886 **Figure Captions**
887
888 Figure 1. Trends in Alewife A) run size for the Monument and Mattapoisett rivers in
889 Massachusetts, B) mean total length (mm) for the Monument River and Stony Brook, C)
890 mean age of female and male Alewives for the Monument River, and D) total mortality
891 rates estimated from a statistical escapement-at-age model for the Monument River stock
892 (Nelson et al., 2011) updated with data from 2011-2015 (ASMFC, 2017).
893
894 Figure 2. Schematic of model processes for the A) juvenile/adult and B) egg, yolk-sac, post-
895 larval/young-of-the-year sub-models. *M* is natural mortality, *CC* is carrying-capacity
896 mortality, and ΔL is change in body length (growth).

897 Figure 3. Plots of Morris σ versus Morris μ for six output variables: run size, adult mean lengths
898 in the river, run sex ratio, total egg abundance, YOY abundance exiting lake, and age-1
899 mean length on May 1.

900 Figure 4. Comparison of model predictions to observed literature and field data for A) first day
901 of run initiation in the Parker River (PR) reported in Cole et al. (1978), Annaquatucket
902 River (AR) reported by Richkus (1974), and multiple rivers observed by Rosset et al.
903 (2017), B) grand mean age (minimum and maximum of mean ages from observed (Cole
904 et al. 1978) and simulated years 1972-1978) of male and female Alewife in the Parker
905 River, C) first day of hatching and D) mean lengths (and 95% percentiles) of age-1
906 Alewife. Note that, although variable, the first day of hatching becomes earlier over time
907 as a result of increasing water temperatures (see Supplemental Document Section 15-17).

908 Figure 5. Derived mortality rates used in the three simulation scenarios. Bycatch mortality
909 represents the annual exploitation fraction, and those for in-river harvest and Striped Bass
910 represent daily fractions.

911 Figure 6. Simulated run size, run mean total length of adults and run mean age of females for the
912 three hypotheses examined. Observed data from the Monument River only are shown.
913 See Figure 1 from data from other rivers. Predictions are averages of 75 simulations.

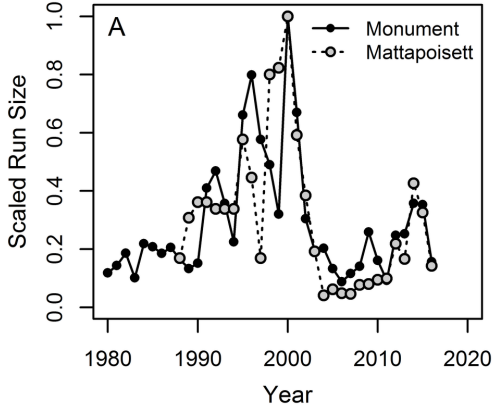
A
Monument
Mattapoisett
Scaled Run Size
0.0
0.2
0.4
0.6
0.8
1.0
1980
1990
2000
2010
2020
Year

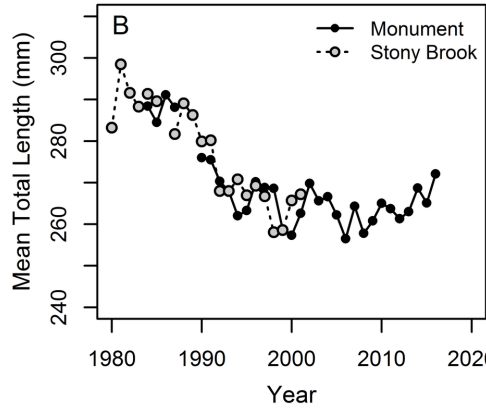
B
Monument
Stony Brook
Mean Total Length (mm)
240
260
280
300
1980
1990
2000
2010
2020
Year

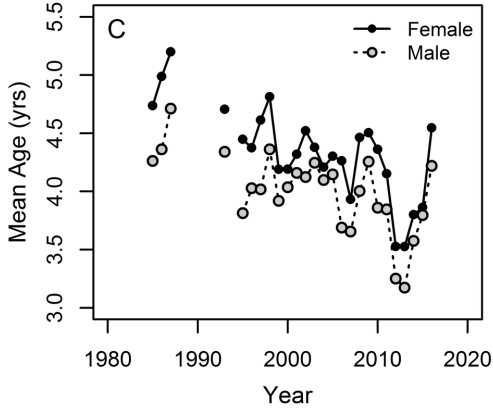
C
Female
Male
Mean Age (yrs)
3.0
3.5
4.0
4.5
5.0
5.5
1980
1990
2000
2010
2020
Year

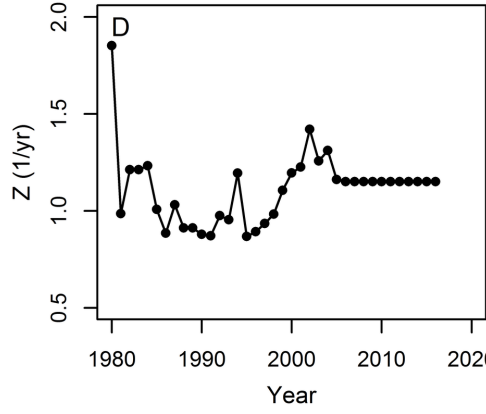
D
Z (1/yr)
0.5
1.0
1.5
2.0
1980
1990
2000
2010
2020
Year

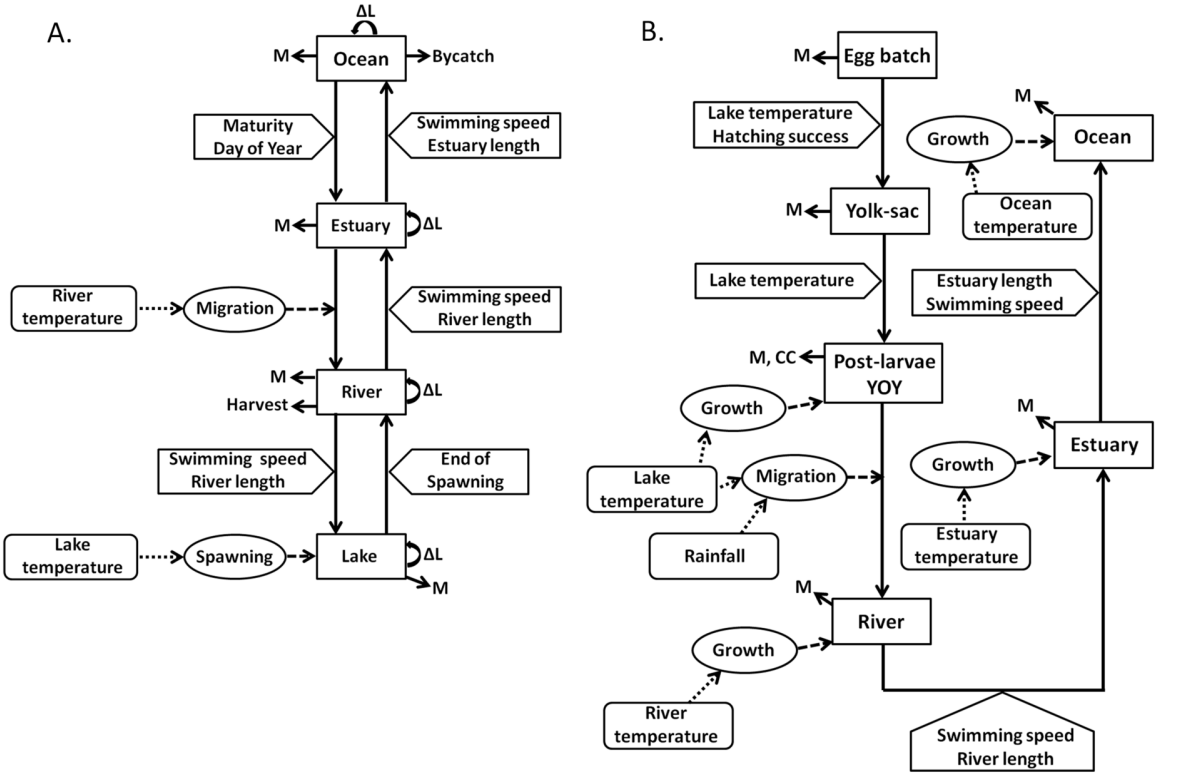
A.
ΔL
M
Ocean
Bycatch
Maturity
Day of Year
Swimming speed
Estuary length
M
Estuary
ΔL
River
temperature
Migration
Swimming speed
River length
M
Harvest
River
ΔL
Swimming speed
River length
End of
Spawning
Lake
temperature
Spawning
Lake
ΔL
M
B.
M
Egg batch
Lake temperature
Hatching success
Growth
M
Ocean
Ocean
temperature
M
Yolk-sac
Lake temperature
Estuary length
Swimming speed
M, CC
Post-larvae
YOY
Growth
M
Estuary
Lake
temperature
Migration
Growth
Rainfall
Estuary
temperature
M
River
Growth
River
temperature
Swimming speed
River length

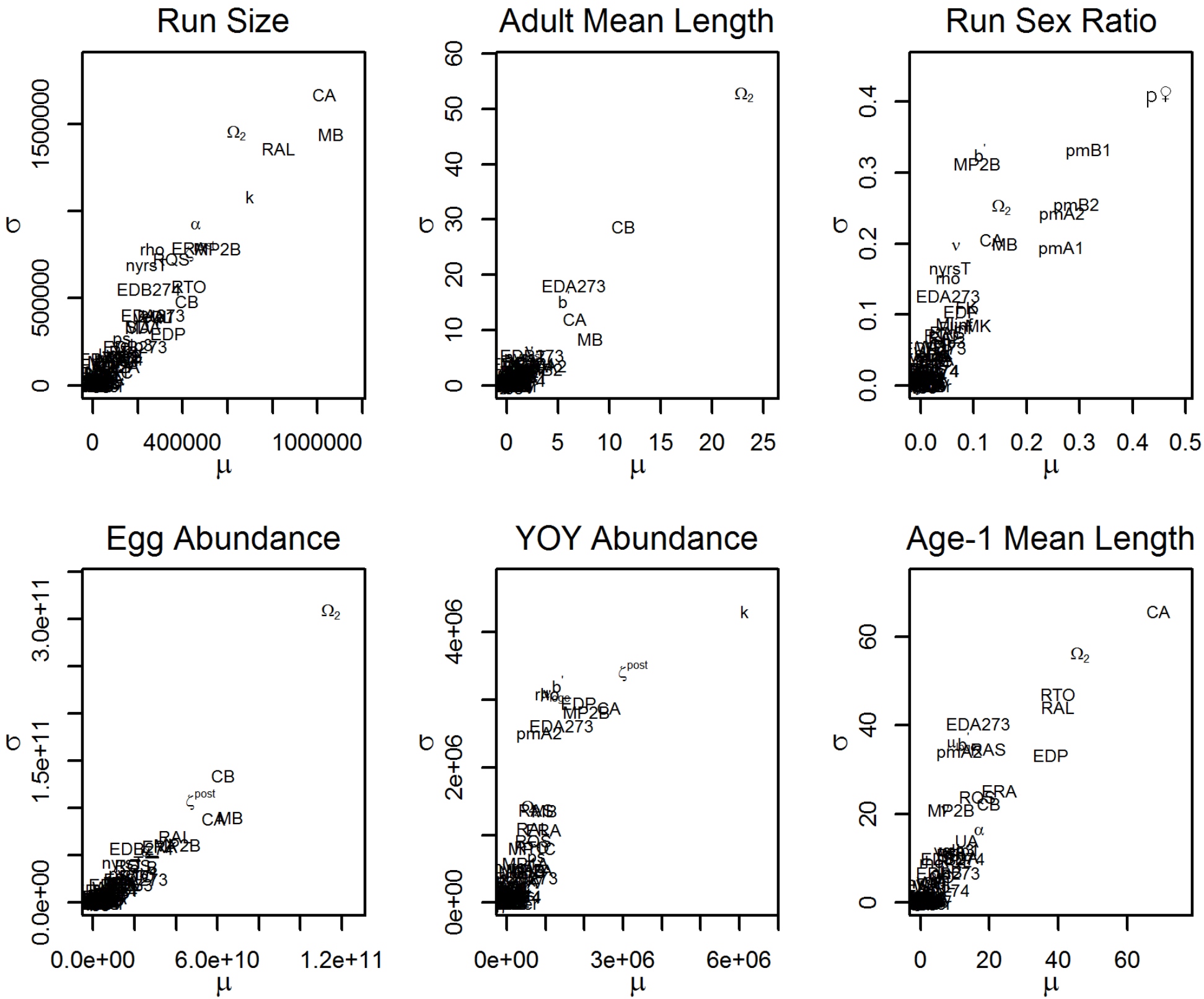
Run Size
σ
μ
0
500000
1500000
0
400000
1000000
CA
MB
Ω2
RAL
k
α
rho
MP2B
RQS
nyrsT
EDB274
RTO
CB
EDP
Adult Mean Length
σ
μ
0
10
20
30
40
50
60
0
5
10
15
20
25
Ω2
CB
EDA273
b
CA
MB
Run Sex Ratio
σ
μ
0.0
0.1
0.2
0.3
0.4
0.0
0.1
0.2
0.3
0.4
0.5
p♀
b'
MP2B
pmB1
Ω2
pmB2
pmA2
ν
CA
MB
pmA1
nyrsT
rho
EDA273
EDP
MK
Egg Abundance
σ
μ
0.0e+00
1.5e+11
3.0e+11
0.0e+00
6.0e+10
1.2e+11
Ω2
CB
ζpost
CA
MB
RAL
MP2B
YOY Abundance
σ
μ
0e+00
2e+06
4e+06
0e+00
3e+06
6e+06
k
ζpost
b'
rho
EDP
CA
MP2B
EDA273
pmA2
Age-1 Mean Length
σ
μ
0
20
40
60
0
20
40
60
CA
Ω2
RTO
RAL
EDA273
b'
pmA2
RAS
EDP
ERA
RQS
CB
MP2B
α
UA

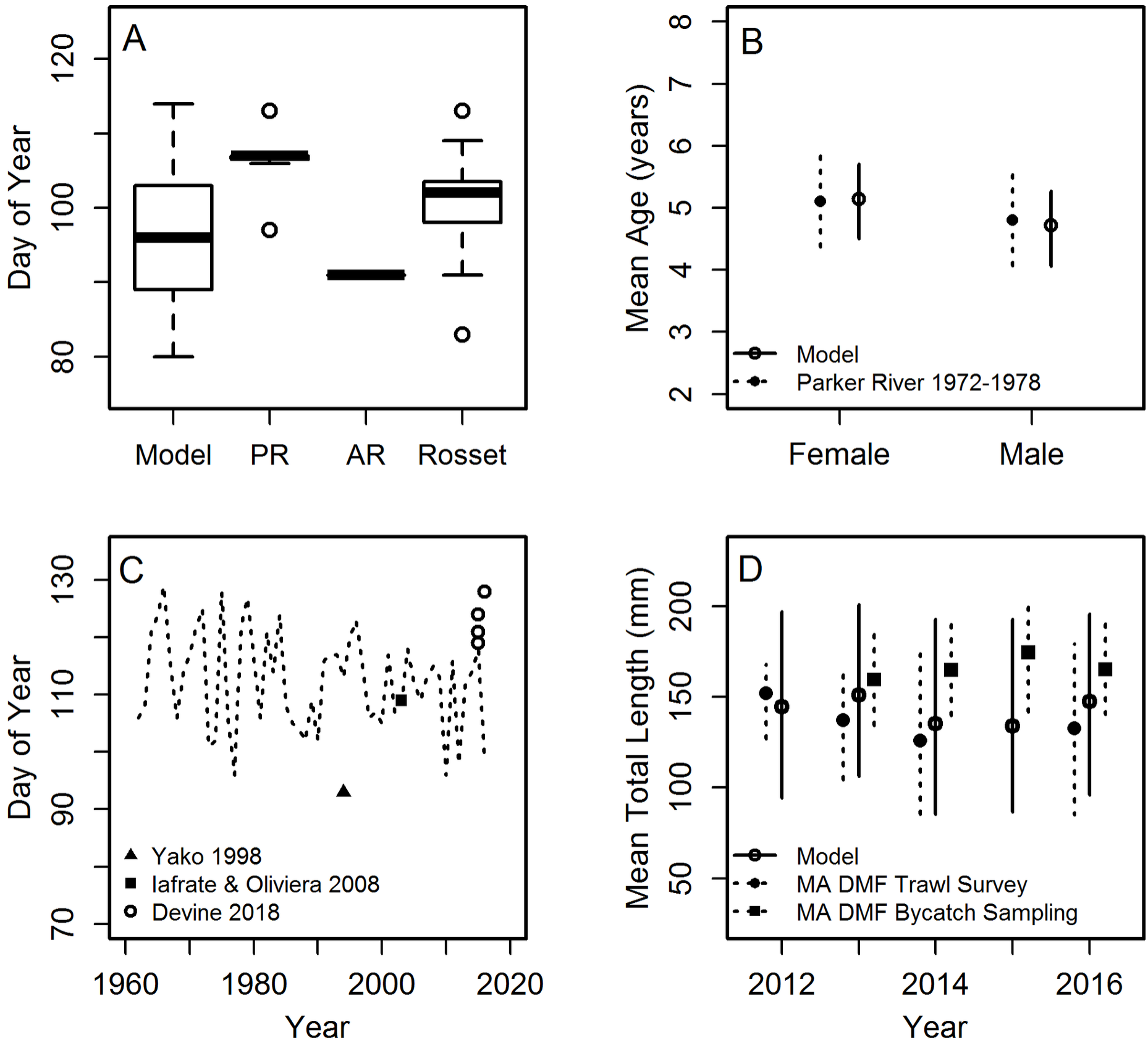
A
Day of Year
80
100
120
Model
PR
AR
Rosset
B
Mean Age (years)
2
3
4
5
6
7
8
Model
Parker River 1972-1978
Female
Male
C
Day of Year
70
90
110
130
Yako 1998
Iafrate & Oliviera 2008
Devine 2018
1960
1980
2000
2020
Year
D
Mean Total Length (mm)
50
100
150
200
Model
MA DMF Trawl Survey
MA DMF Bycatch Sampling
2012
2014
2016
Year

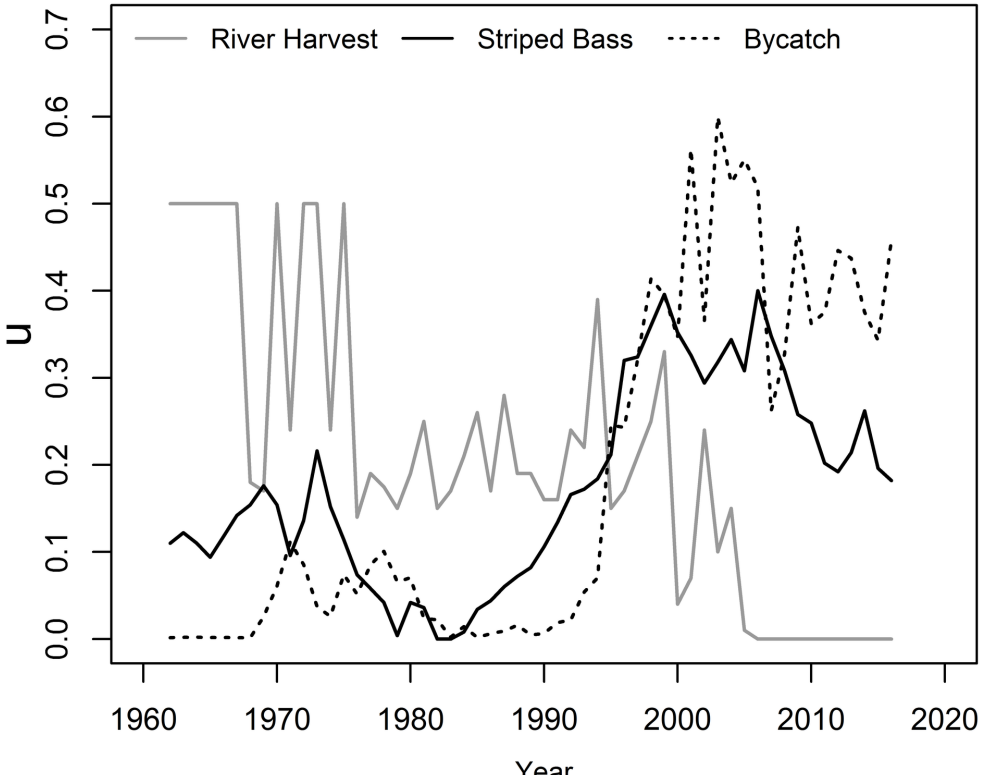
River Harvest
Striped Bass
Bycatch
u
0.0
0.1
0.2
0.3
0.4
0.5
0.6
0.7
1960
1970
1980
1990
2000
2010
2020
Year

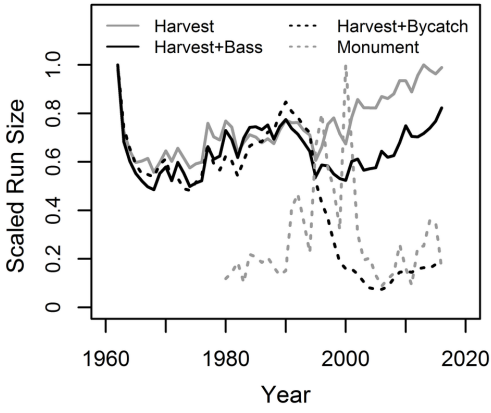
Harvest
Harvest+Bass
Harvest+Bycatch
Monument
Scaled Run Size
0
0.2
0.4
0.6
0.8
1.0
1960
1980
2000
2020
Year

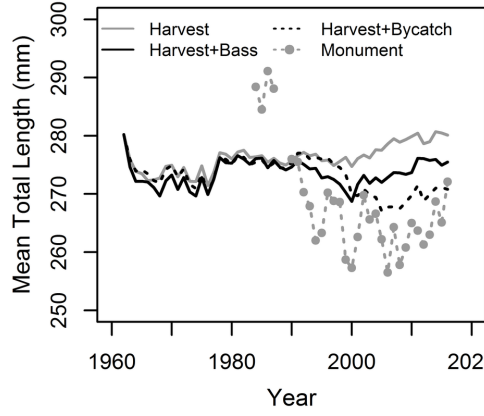
Harvest
Harvest+Bass
Harvest+Bycatch
Monument
Mean Total Length (mm)
250
260
270
280
290
300
1960
1980
2000
2020
Year

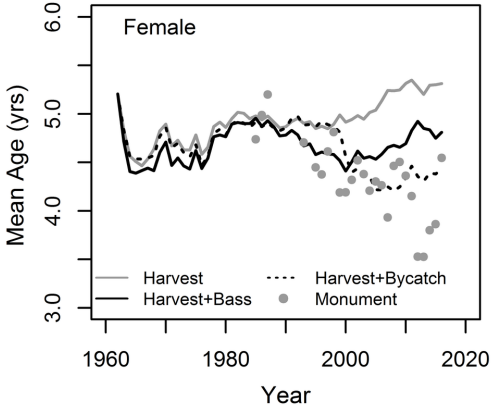
Female
Harvest
Harvest+Bass
Harvest+Bycatch
Monument
Mean Age (yrs)
3.0
4.0
5.0
6.0
1960
1980
2000
2020
Year

Table 1. Description of Indexes used in the mathematical equations

Index	Definitions	Range
d	Day of year	{1,..,365}
p	Platoon	{1,..,100}
a	Age	{1,..,9+}
r	Region	{1=Ocean, 2=Estuary, 3=River, 4=Lake}
x	Sex	{1=Female, 2=Male}
m	Maturity	{1=Immature, 2=Mature}
f	Fleet	{1=Bottom Trawl, 2=Mid-Water}
b	Daily Egg Batch	$\{d(E_d),..,d(E_{last})\}$

Table 2. Definitions of symbols used in the mathematical description of the Alewife juvenile/adult simulation sub-model.

Symbol s	Definitions
D	Number of days in the year (365)
$N^r_{d,p,a,x,m}$	Numbers of platoon *p*, age *a*, sex *x* and maturity *m* individuals at the beginning of day *d* in region *r*
M^r_p, MA, MB, δ_r	Daily instantaneous natural mortality rate (d^{-1}) for platoon *p* in region *r*, intercept and exponent of mortality equation, *M* multiplier for region *r*
μ, F_d	Annual fraction of by-catch mortality, daily instantaneous fishing mortality
$L_{d,x,p}$	Total length (mm) of platoon *p* of sex *x* on day *d*
η_n, D_n	Fraction of by-catch *F* occurring in month *n*, number of days in month *n*
P_f	The annual fraction of bycatch attributed to fleet *f* (P_2=1-P_1)
$s_{p,f}$	The selectivity at length platoon *p* in region 1 by fleet *f* (see Supplementary Document Section 1)
$\Delta L_{d,x,p}, L\infty_x, K_x, t0_x$	Growth increment (mm/day) of platoon *p* and sex *x* on day *d*, sex-specific von Bertalanffy growth equation parameters
$L^o_{x,p}, g_d, gA, gB, gC$	Length of sex *x* and platoon *p* on day 1, fraction of annual growth increment, sine function parameters
ES	Estuary entrance day
$rT, ndaysT$	Temperature for initiation of run start (°C), number of prior days used in calculation
$H, PRED$	Fraction of Alewife run that is harvested, fraction of run eaten by a predator
$\theta_d, a', b', crl, c'$	Daily fraction of platoon numbers immigrating to river, first day of immigration, peak day of immigration, run length, last day of immigration $(a' + crl)$
$\sigma^2_\varepsilon, \rho$	Normal variance for run error sampling, first-order autocorrelation
$rdur, rl, edur, el, v, \bar{s}$	Days spent in river, river length, days spent in estuary, estuary length, swimming speed (body length/sec), mean body size
$sdur, lA, lB, pdays, lC$	Spawning duration (days), intercept of spawning duration equation, slope of spawning duration equation, day of year after initiation of emigration expressed as a proportion of run duration, value of *sdur* for *pdays*<0.45
$CV_{sdur}, spdday$	Coefficient of variation for *sdur* calculation, added delay before spawning begins
$sT, Bdur$	Lower spawning temperature limit (°C), days between batches
$\bar{W}_p, \bar{B}, WA, WB, \bar{e}, E_d$	Mean weight of females of platoon *p* (grams), mean number of egg batches produced per female, intercept of length-weight equation, slope of length-weight equation, mean total number of eggs per gram produced per females , total number of eggs produced by spawning females on day *d*
$pm_{x,a,p}, pmA_x, pmB_x$	*pm* is the proportion of mature fish of sex *x*, age *a* and length platoon *p,* intercept of sex *x* maturity equation, slope of sex *x* maturity equation

Table 3. Equations describing dynamics and processes of the juvenile/adult sub-model.

$N^r_{d,p,a,x,m} = N^r_{d-1,p,a,x,m} e^{-\sum s_{p,f} F_{d-1,f} - M^r_p \delta^r}, r = 1$	JA.1
$F_{d,f} = ((-loge(1-\mu)\eta_n)/D_n)P_f$	JA.2
$M^r_p = (MA \cdot L^{MB}_p)/D$	JA.3
$N^r_{d,p,a,x,2} = N^r_{d-1,p,a,x,2} e^{-M^r_p \delta^r}, r = 2,4$	JA.4
$N^r_{d,p,a,x,2} = N^r_{d-1,p,a,x,2}(1-H)(1-PRED)e^{-M^r_p \delta^r}, r = 3$	JA.5
$L_{d,x,p} = L_{d-1,x,p} + \Delta L_{d-1,x,p}$	JA.6
$\Delta L_{d,x,p} = \left(L_{\infty,x} - L^o_{x,p}\right) \cdot (1 - e^{-Kx}) \cdot g_d$	JA.7
$g_d = gA + gB * sin\left(2\pi \cdot \frac{d - gC}{D}\right) / \sum_{d=1}^{D} gA + gB * sin\left(2\pi \cdot \frac{d - gC}{D}\right)$	JA.8
$N^3_{d,p,a,x,2} = N^2_{d,p,a,x,2} \cdot \theta_d$	JA.9
$N^2_{d,p,a,x,2} = N^2_{d,xp,a,x,2} \cdot (1 - \theta_d)$	JA.10
$p_d = \begin{cases} 2(d-a')/[(c'-a')(b'-a')], & d \le b' \\ 2(c'-d)/[(c'-a')(c'-b')] \ , & d > b' \end{cases}$	JA.11
$p^*_d = \begin{cases} if\ d = a', p_d \exp^{\varepsilon^*_d} \ \ where\ \ \varepsilon^*_d = N(0, \sigma^2_\varepsilon) \\ if\ d > a', p_d \exp^{\varepsilon^*_d - \sigma^2_\varepsilon/2} \ \ where\ \ \varepsilon^*_d = \varepsilon^*_{d-1} \cdot \rho + \sqrt{1-\rho^2} \cdot N(0, \sigma^2_\varepsilon) \end{cases}$	JA.12
$p'_d = p^*_d / \sum_{d=a'}^{c'} p^*_d$	JA.13
$\theta_d = p'_d / \sum_{d}^{c'} p'_d$	JA.14
$rdur = \begin{cases} 1, if\ \ rl/(v\bar{s} \cdot 0.0864) < 1 \\ round(rl/(v\bar{s} \cdot 0.0864), 0), if\ \ rl/(v\bar{s} \cdot 0.0864) > 1 \end{cases}$	JA.15
$sm = \begin{cases} e^{lA \cdot (pdays - lB)}, pdays \ge 0.45 \\ lC \qquad\qquad\quad , pdays < 0.45 \end{cases}$	JA.16
$sdur = e^{LN(sm, (CV_{sdur} \cdot sm)^2)}$	JA.17
$E_d = \sum_a \sum_p (\bar{W}_p \bar{e}/\bar{B}) \cdot N^4_{d,p,a,1,2}$	JA.18
$\bar{W}_p = 10^{WA + WB \log_{10} Lp}$	JA.19
$pm_{x,a,p} = e^{pmA_x + pmB_x \cdot L_{x,a,p}} / (1 + e^{pmA_x + pmB_x \cdot L_{x,a,p}})$	JA.20

Table 4. Definitions of symbols used in the mathematical description of the egg, yolk-sac larvae, post-larvae/YOY sub-model.

Symbols	Definitions
nb	Number of daily egg batches
$N_{b,d}^{Eggs}, N_{b,d}^{Yolksac}$	Number of eggs in batch *b* on day *d*, number of yolk-sac larvae from batch *b* on day *d*
M^{Eggs}, ζ^{Eggs}	Daily instantaneous natural mortality rate for eggs, M multiplier for eggs
$h_d, d(b), d(h), o_d$	Egg hatching time (days) at temperature on day *d*, day batch of eggs is laid, day eggs hatch, fraction of eggs that successfully hatch at temperature (°C) on day d
dhA, dhB	Hatching time-temperature equation parameters
oA, oB, oC	Hatching success –temperature equation parameters
$M^{Yolksac}, \zeta^{Yolksac}$	Daily instantaneous natural mortality rate for yolksac larvae, M multiplier for yolksac larvae
$y_d, d(y)$	Yolksac absorption time (days) at temperature on day *d,* day yolksac is fully absorbed
dyA, dyB	Yolksac absorption-temperature equation parameters
T_d	Water temperature (°C) on day d
$N_{b,d,p}^{Post,r}$	Number of post-larvae in platoon *p* from batch *b* on day *d* in region *r*
l, A, k, k_b	Post-larval capacity (larvae per km^2), lake area (km^2), carrying capacity, batch carrying capacity
$\pi_{b,p}^{Post}, L_p^{Post}, \Delta L_p^{Post}$	Proportion of post-larvae from batch *b* in length platoon *p*, total length (mm) of post-larvae in platoon *p*, the daily increment of length increase
σ^2	variance of $\bar{L}^{Post}$
$L_{\min}, L_{\max}, \mu_{\log e}, np$	Minimum length, maximum length, mean length (natural log scale), number of post-larvae length platoons
$M_{b,d,p}^{Post}, \zeta_{r,1}^{Post}, \zeta_{r,2}^{Post}$	Daily instantaneous natural mortality rate for post-larvae/YOY of batch *b* and platoon *p* on day *d*, regional M multipliers for post-larvae $\leq$22 mm TL and >22 mm TL
$ml, d(s), d(e)$	Post-larvae emigration length, day on which $L_p^{Post} \geq ml$, last day of emigration
ψ_d, τ_d	Probability of emigration based on temperature at start of day d, proportion emigrating on day d
$V, velp1, velp2, velp3$	Swimming speed (cm/sec), equation parameters
$\bar{W}_p^{Post}$	Mean weight (g) of platoon *p* derived from bioenergetics model
ϖ_r	River and estuary duration multiplier

Table 5. Equations describing dynamics and processes of the egg-YOY sub-model.

$$N_{b,d}^{Eggs} = N_{b,d-1}^{Eggs} e^{-M^{Eggs}\zeta^{Eggs}}$$ EY.1

$$h_d = dhA \cdot (1.8T_d + 32)^{-dhB}$$ EY.2

$$d(h) = \sum_{j=d(b)}^{d-1} \frac{1}{h_j} \geq 1$$ EY.3

$$o_d = (oA + oB(1.8T_d + 32) - oC \cdot (1.8T_d + 32)^2)/100$$ EY.4

$$N_{b,d}^{Yolksac} = \begin{cases} N_{b,d-1}^{Eggs} e^{-M^{Eggs}\zeta^{Eggs}} o_{d-1}, & d = d(h) \\ N_{b,d-1}^{Yolksac} e^{-M^{Yolksac}\zeta^{Yolksac}}, & d > d(h) \end{cases}$$ EY.5

$$y_d = dyA \cdot T_d^{dyB/T_d}$$ EY.6

$$d(y) = \sum_{j=d(h)}^{d-1} \frac{1}{y_j} \geq 1$$ EY.7

$$N_{b,d(y)}^{Post,4} = N_{b,d-1}^{Yolksac} e^{-M^{Yolksac}\zeta^{Yolksac}}, d = d(y)$$ EY.8

$$k_b = k/nb$$ EY.9

$$N_{b,d}^{Post,4} = \begin{cases} k_b, & N_{b,d}^{Post,4} \geq k_b \\ N_{b,d}^{Post,4}, & N_{b,d}^{Post,4} < k_b \end{cases}$$ EY.10

$$L_p^{Post} = \begin{cases} L_{\min}, & p = 1 \\ L_{p-1}^{Post} + \dfrac{L_{\max} - L_{\min}}{np - 1}, & p > 1 \& p < np \\ L_{\max}, & p = np \end{cases}$$ EY.11

$$f(L_p^{Post}) = 1/L_p^{Post}\sigma\sqrt{2pi} \cdot \exp(-(\log_e L_p^{Post} - \mu_{\log_e})^2/2\sigma^2)$$ EY.12

$$\pi_{b,p}^{Post} = f(L_p^{Post}) / \sum_{p=1}^{np} f(L_p^{Post})$$ EY.13

$$N_{b,d,p}^{Post,4} = multinomial(\pi_{b,p}^{Post}, N_{b,d}^{Post,4})$$ EY.14

$$N_{b,d,p}^{Post,r} = N_{b,d-1,p}^{Post,r} e^{-M_{d-1,p}^{Post}\zeta^{Post}}$$ EY.15

Table 5 cont.

$$M_{d,p}^{Post} = \begin{cases} MP1A \cdot \exp^{MP1B*T_d} (L_p^{Post})^{-MP1C} \zeta_{r,1}^{Post}, & L_p^{Post} \le 22\ mm\ \ TL, \\ (MP2A \cdot (L_p^{Post})^{-MP2B})/D\zeta_{r,2}^{Post}, & L_p^{Post} > 22\ mm\ \ TL \end{cases} \quad \text{EY.16}$$

$$N_{b,d,p}^{Post,3} = \frac{\psi_d \tau_d}{\sum_d^{d(e)} \psi_d \tau_d} N_{b,d,p}^{Post,4}, \text{where} L_p^{Post} > ml \quad \text{EY.17}$$

$$\psi_{d \ge d(s)} = \begin{cases} 1, & \frac{\exp^{uA-uB \cdot T_d}}{1+\exp^{uA-uB \cdot T_d}} \ge 0.5 \\ 0, & \frac{\exp^{uA-uB \cdot T_d}}{1+\exp^{uA-uB \cdot T_d}} < 0.5 \end{cases} \quad \text{EY.18}$$

$$n_d = \begin{cases} NB(1, mu = 10.71, size = 0.244), \text{rainfall} < 18mm \\ N(1, mean = 473, sd = 183.05), \quad \text{rainfall} \ge 18mm \\ NB(1, mu = 10.71, size = 0.244), \quad d > 285 \end{cases} \quad \text{EY.19}$$

$$\tau_d = n_{d-1} / \sum_{j=d-1}^{d(e)-1} n_{j-1} \quad \text{EY.20}$$

$$N_{b,d,p}^{Post,4} = N_{b,d,p}^{Post,4} - N_{b,d,p}^{Post,3} \quad \text{EY.21}$$

$$V = velp1 \cdot \bar{W}_p^{Post^{velp2}} e^{velp3 \cdot T_d} \quad \text{EY.22}$$

$$rdur = \begin{cases} 1, & V/8.64e9/rl \cdot \varpi_3 < 1 \\ round(V/8.64e9/rl \cdot \varpi_3, 0), & V/8.64e9/rl \cdot \varpi_3 \ge 1 \end{cases} \quad \text{EY.23}$$

$$edur = \begin{cases} 1, & V/8.64e9/el \cdot \varpi_2 < 1 \\ round(V/8.64e9/el \cdot \varpi_2, 0), & V/8.64e9/el \cdot \varpi_2 \ge 1 \end{cases} \quad \text{EY.24}$$

Table 6. Definitions of symbols used in the mathematical description of bioenergetics sub-model.

Symbol	Definitions
WAS, WBS	For $L_p \leq 22\ mm\ TL$, intercept and coefficient for length-weight equation
WAL, WBL	For $L_p > 22\ mm\ TL$, intercept and coefficient for length-weight equation
$C_p, C_{\max}$	Consumption rate of platoon *p* (g/g/day), maximum feeding rate (g/g/day)
$pr_p, ps, \alpha, \alpha', \beta', \Omega_r$	Proportion of maximum consumption for platoon *p*, base proportion maximum consumption, intercept of *pr* versus length equation, intercept of *pr* versus density equation, slope of *pr* versus density equation, regional growth multiplier
$f(TC), f(TR)$	Temperature dependence function for consumption, respiration
KA, KB	Increasing portion of temperature dependence function, decreasing portion of temperature dependence function
EDP	Energy density of prey (joules/g)
CA, CB	Intercept and exponent of mass dependence function
$CQ, CK1$	Temperature at which temperature dependence is a small fraction of the maximum rate, temperature dependence parameter
$CTO, CK4$	Water temperature corresponding to 0.98 of the maximum consumption rate, temperature dependence parameter
CTL, CTM	Temperature at which dependence is some reduced fraction of $CK4$ of the maximum rate, temperature at which dependence is still 0.98 of the maximum
R_p	Specific rate of respiration (joules/g/day)
RAS, RBS, RQS	For $L_p \leq 49\ mm\ TL$, intercept of mass function (g/g/day), slope of mass function, approximates the Q10 (1/°C)
RAL, RBL, RQL	For $L_p > 49\ mm\ TL$, intercept of mass function (g/g/day), slope of mass function, approximates the Q10 (1/°C)
ACT, VEL	Activity multiplier as a function swimming speed, swimming speed (cm/sec)
RTO	Coefficient for swimming speed dependence on metabolism (sec/cm)
$RK1, RK4, RTL$	Intercept for swimming speed above cutoff temperature (cm/sec), mass dependence coefficient for swimming speed at all water temperatures, cutoff temperature at which the activity relationship changes (°C)
$AM, BACT$	Intercept for swimming speed versus mass relationship at temperature<RTL (cm/sec for a 1 gram fish at 0°C), water temperature dependence coefficient of swimming speed at temperatures below RTL(1/°C)
OC	Oxycalorific coefficient used to convert grams to joule equivalents
ER_p, ERA	Egestion rate (g/g/day) of platoon *p*, constant proportion of *C*
U_p, UA, S_p, SDA	Excretion (joules/g/day), constant proportion of assimilated energy, proportion assimilated energy lost to specific dynamic action, specific dynamic action
ED, EDA_d, EDB_d	Energy density of Alewife (joules/g), intercept of length-ED relationship for day *d*, slope of length-ED relationship for day *d*
$\tilde{T}_p, Ta, Tb, Tc$	Optimal temperature (°C) for platoon *p*, asymptote parameters for optimal temperature versus platoon length equation

Table 7. Equations describing the bioenergetics sub-model.

$$\bar{W}_p = \begin{cases} e^{WAS+WBS\cdot\log e(Lp)}, L_p \le 22\ mm\ TL, \\ e^{WAL+WBL\cdot\log e(Lp)}, L_p > 22\ \ mm\ TL, \end{cases} \quad \text{BE.1}$$

$$C_p = C_{max,p} \cdot EDP \cdot pr_p \cdot f(T_d) \quad \text{BE.2}$$

$$C_{max,p} = \begin{cases} 0.8464, & \bar{W}_p\ < 1\ g \\ CA \cdot \bar{W}_p^{CB}, & \bar{W}_p\ \ge 1\ g \end{cases} \quad \text{BE.3}$$

$$pr_p = \begin{cases} ps \cdot \Omega_r, L_p \le 22mm\ TL \\ (\alpha + \beta \cdot L_p) \cdot \Omega_r, L_p > 22mmTL \end{cases} \quad \text{BE.4}$$

$$\beta = \begin{cases} 0.0021, & \alpha' + \beta' / \sum_b N_{b,d}^{Post,4} < 0.0021 \\ \alpha' + \beta' / \sum_b N_{b,d}^{Post,4}, & 0.0021 \le \alpha' + \beta' / \sum_b N_{b,d}^{Post,4} \le 0.0026 \\ 0.0026, & \alpha' + \beta' / \sum_b N_{b,d}^{Post,4} \ge 0.0026 \end{cases} \quad \text{BE.5}$$

$$f(T_d) = KA \cdot KB \quad \text{BE.6}$$

$$KA = \frac{CK1 \cdot L_1}{(1 + CK1(L_1 - 1)} \quad \text{BE.7}$$

$$L1 = \exp^{G_1 \cdot (T_d - CQ)} \quad \text{BE.8}$$

$$G_1 = \frac{1}{CTO - CQ} \ln\left(\frac{0.98(1 - CK1)}{CK1 \cdot 0.02}\right) \quad \text{BE.9}$$

$$KB = \frac{CK4 \cdot L_2}{1 + CK4(L_2 - 1)} \quad \text{BE.10}$$

$$L_2 = \exp^{G_2(CTL - T_d)} \quad \text{BE.11}$$

$$G_2 = \frac{1}{CTL - CTM} \ln\left(\frac{0.98(1 - CK4)}{CK4 \cdot 0.02}\right) \quad \text{BE.12}$$

$$R_p = \begin{cases} RAS(\bar{W}_p^{Post})^{RBS} \cdot ACT \cdot f(TR)_d \cdot OC, & Lp \le 49\ mm\ TL \\ RAL(\bar{W}_p^{Post})^{RBL} \cdot ACT \cdot f(TR)_d \cdot OC, & Lp > 49\ mm\ TL \end{cases} \quad \text{BE.13}$$

$$ACT = \begin{cases} 1, L_p \le 49\text{mmTL} \\ \exp^{\ \text{RTO}\cdot\text{VEL}}, L_p > 49\text{mmTL} \end{cases} \quad \text{BE.14}$$

$$VEL = \begin{cases} RK1(\bar{W}_p^{Post})^{RK4}, T_d\ > RTL \\ A_m \bar{W}_p^{Post^{RK4}} \exp^{BACT \cdot T_d}, T_d \le RTL \end{cases} \quad \text{BE.15}$$

Table 7 cont.

$f(TR)_d = \exp^{RQ \cdot T_d}$	BE.16
$ER_p = ERA \cdot C_p$	BE.17
$U_p = UA(C_p - ER_p)$	BE.18
$S_p = SDA \cdot (C_p - ER_p)$	BE.19
$\bar{W}_{d,p}^{Post} = \bar{W}_{d-1,p}^{Post} + \Delta B_{d-1,p}$	BE.20
$\Delta B_{d-1,p} = \frac{(C_{d-1,p} - R_{d-1,p} - ER_p - U_p - S_p)}{ED_{d-1,p}} \bar{W}_{d-1,p}^{Post}$	BE.21
$ED_{d,p} = \begin{cases} EDA1 + EDB1 \cdot L_{d,p}, d \leq 273 \\ EDA2 + EDB2 \cdot L_{d,p}, d > 273 \end{cases}$	BE.22
$L_{d,p} = \begin{cases} e^{(\log e(\bar{W}_{d,p}^{Post}) + WAS)/WBS}, L_{d-1,p} \leq 22\ mm\ TL \\ e^{(\log e(\bar{W}_{d,p}^{Post}) + WAL)/WBL}, L_{d-1,p} > 22\ mm\ TL \end{cases}$	BE.23
$\tilde{T}_p = \begin{cases} T_a/(1 + e^{T_b + T_c L_p}), & L_p < 42\ mm\ TL \\ 18.2, & L_p \geq 42\ mm\ TL \end{cases}$	BE.24

Table 8. Results of Morris sensitivity analysis showing the top-twenty μs for six output variables. TL = total length (mm) and N = abundance. See Figure 3 for more details.

Parameter	Run Size	Parameter	Adult Mean TL	Parameter	Sex Ratio	Parameter	Egg N	Parameter	YOY N	Parameter	Age-1 Mean TL
MB	1060136	Ω_2	23.14	$p_{♀}$	0.448	Ω_2	1.14E11	*k*	6129498	*CA*	68.99
CA	1032472	*CB*	11.34	*pmB1*	0.317	*MB*	6.60E10	ξ_1	3262671	Ω_2	46.27
RA50	826973	*MB*	8.10	*pmB2*	0.293	*CB*	6.29E10	*CA*	2637403	*RTO*	39.91
k	698598	*CA*	6.64	*pmA2*	0.267	*CA*	5.81E10	*MP2B*	2046166	*RAL*	39.89
Ω_2	639013	*EDA273*	6.53	*pmA1*	0.266	ξ_1	5.18E10	*EDP*	1848882	*EDP*	37.70
MP2B	555478	*b'*	5.56	*MB*	0.159	*MP2B*	4.05E10	*EDA273*	1414878	*ERA*	22.89
ξ_1	475550	*pmA2*	3.65	Ω_2	0.152	*RAL*	3.96E10	*b'*	1321743	*CB*	19.85
α	457451	*pmB2*	3.24	*CA*	0.133	*k*	3.82E10	μ_{loge}	1244198	*RAS*	19.77
ERA	430475	*EDB273*	2.46	*b'*	0.112	*ERA*	3.21E10	*ρ*	1040644	*α*	16.95
RTO	428328	*ERA*	2.30	K_2	0.109	$\bar{B}$	2.84E10	*v*	1032588	*EDA273*	16.83
CB	417892	*v*	2.18	*MP2B*	0.107	*α*	2.55E10	*MB*	968857	*RQS*	16.58
RQS	348760	ξ_1	2.08	K_1	0.086	*EDB274*	2.32E10	*ERA*	954126	*UA*	13.52
EDP	333956	*ndaysT*	1.78	*EDP*	0.077	*velp1*	2.17E10	*pmA1*	833169	*b'*	12.43
RQL	276194	*pmA1*	1.72	*v*	0.067	*RTO*	2.11E10	*ps*	767496	μ_{loge}	12.03
velp1	275004	*MP2B*	1.61	$L_{\infty,1}$	0.065	*EDA273*	2.07E10	*RAS*	750182	*SDA*	11.76
UA	269654	*pmB1*	1.60	$L_{\infty,2}$	0.063	$\bar{e}$	1.99E10	*RQS*	682251	*pmA2*	11.29
EDA273	266816	*dhB*	1.59	*nyrsT*	0.055	*RQS*	1.94E10	*RAL*	680269	*velp1*	11.20
ρ	263594	*EDB274*	1.51	*ρ*	0.052	*EDP*	1.56E10	*MP1C*	650904	*velp3*	9.85
EDB274	248770	*RQS*	1.50	*EDA273*	0.051	*UA*	1.46E10	*RTO*	647212	*RQL*	9.84
ndaysT	239476	*RAL*	1.49	*RAS*	0.050	*RQL*	1.44E10	Ω_2	615851	*RBL*	9.44